FINITE ELEMENT FORMULATION OF MODERATELY LARGE AMPLITUDE MEMBRANE FLUTTER AT LOW SPEEDS

By

HANUMAN

DEPARTMENT OF AERONAUTICAL ENGINEERING

INDIAN INSTITUTE OF TECHNOLOGY KANPUR

AUGUST 1973

FINITE ELEMENT FORMULATION OF MODERATELY LARGE AMPLITUDE MEMBRANE FLUTTER AT LOW SPEEDS

A Thesis Submitted
In Partial Fulfilment of the Requirements
for the Degree of
MASTER OF TECHNOLOGY

By
HANUMAN

to the

DEPARTMENT OF AERONAUTICAL ENGINEERING
INDIAN INSTITUTE OF TECHNOLOGY KANPUR

AUGUST 1973

CERTIFICATE

This is to certify that the work 'FINITE ELEMENT FORMULATION OF MODERATELY LARGE AMPLITUDE MEMBRANE FLUTTER AT LOW SPEEDS' has been carried out under my supervision and has not been submitted elsewhere for a degree.

P. N. Murthy

(P.N. MURTHY)
Professor
Department of Aeronautical Engineering
Indian Institute of Technology Kanpur

ACKNOWLEDGEMENTS

To Professor P.N. Murthy who suggested this problem and introduced the finite element method to me. My grateful thanks to him for his invaluable guidance, continuous encouragement and inspiration during the course of this work.

To Dr. N.G.R. Iyengar for his helpful advice whenever sought.

To Mr. D.P. Mazumdar with whom I had very useful discussions from time to time.

To Mr. R.K. Banta who had almost always been with me in ideas, discussions and experiments. My sincere thanks to him for giving critical checks at various stages.

To Hindustan Aeronautics Limited who provided the financial assistance during my second year stay in M.Tech. programme.

Finally, to Mr. S.K. Behl who typed the manuscript with great patience.

Hanuman

ABSTRACT

An analytical formulation for moderately large amplitude travelling wave membrane flutter in incompressible flow has been attempted here using finite element method. The flow has been assumed to take place on both upper and lower surfaces of the membrane having flexible boundaries. The analysis has been made with the assemblage of 16 rectangular elements using the 12-parameter non-conforming model. Hermite polynomials of first order have been used as interpolation functions. An expression for the lateral deflection, representing the travelling wave behaviour for the entire membrane in the global set, has been used. The inplane tension effect and the non-linearity due to large deflections has been considered through the derivation of the geometric stiffness matrix. Small perturbation theory applied to the non-circulatory incompressible flow past the oscillating membrane has been used to give the aerodynamic loading. An aerodynamic matrix, which is kinematically consistent with the stiffness and mass matrices has been derived using the virtual work principle. The flutter criterion has been discussed and a method to solve the complex eigenvalue problem has been presented.

TABLE OF CONTENTS

LIST OF FIGURES

NOMENCLATURE

a, b	element dimensions
a_∞	freestream sound speed
$[a_n]$	12x75 transformation matrix
$[A_e]$, $[A]$	12x12 elemental and 75x75 global aerodynamic matrices respectively
c	wave velocity
E	Young's Modulus of elasticity for membrane material
$\{f\}$	12x1 column vector of Hermite polynomials
h	membrane thickness
$[k]$, $[K]$	12x12 elemental and 75x75 global stiffness matrices respectively
$[m]$, $[M]$	12x12 elemental and 75x75 global mass matrices respectively
t	time
U	strain energy
V_a, V	virtual work and freestream airspeed respectively
w	lateral deflection
$\{W\}$, $\{W^*\}$	12x1 elemental and 75x1 global generalised displacement vectors respectively
x, y, z	local co-ordinate system
X, Y, Z	global co-ordinate system
ϕ	disturbance velocity potential and also $= \frac{\partial w}{\partial y}$
ρ, ρ_m	air and membrane material densities respectively

NOMENCLATURE (Contd.)

ω_{c_r}	critical flutter frequency
$\bar{\mu}$	complex eigenvalue
λ, λ^*	wave length and wave number respectively
ν	Poisson's Ratio
$\{\sigma\}$, $\{\epsilon\}$	2x1 stress and strain vectors respectively

CHAPTER 1

INTRODUCTION

1.1 General

During the last one decade or so, there has been much interest in the utilization of aerodynamic surfaces formed of flexible membranes. While sails are the historical example of such surfaces, their applications are also found in other examples such as parawings, parachutes, flexible rotor blades, glider wings using flexible lifting surfaces and possibly the inflatable aerodynamic surfaces which have yet to come into being. The aerodynamics of the flexible surfaces is different from that for rigid surfaces since in the former deformations influence load distributions.

The aerodynamic analysis for the flexible lifting surfaces has received the attention of few investigators (1,2,3). They have established the shapes of these surfaces as a function of tension and free stream dynamic pressure to give the prescribed aerodynamic loadings. It has been found that for a particular value of inplane tension and for a given configuration there exists a free stream dynamic pressure beyond which the membrane becomes unstable and any oscillation becomes divergent. At this stage the flexible surface ceases to serve its function of providing lift or navigating force to the vehicle. Therefore, it becomes

essential to investigate this aspect of dynamic instability, widely known in aeronautical literature as 'flutter'.

In general, flutter is defined as a self excited or unstable oscillation arising out of the simultaneous action of elastic, inertia and aerodynamic forces upon a mass or a system of masses. During this oscillation it has been shown that the body extracts energy from the airstream. Apart from the flutter of lifting surfaces, this phenomenon is observed in certain non-lifting surfaces also as in case of flags, sails, suspension bridges, electrical transmission lines, skin panels forming external surface of aircraft and missiles etc. The flutter of skin panels, generally termed as 'Panel Flutter' is a local dynamic instability of a panel or group of panels of the exposed surface of the vehicle and is thus distinct from the flutter of a lifting surface or vehicle as a whole.

The flutter encountered in flags, sails, parawings etc. is also included in the study of panel flutter where the membrane acts as a panel. In these cases because of the nature of boundaries and high flexibility of the structure, it is quite likely that flutter can occur even in incompressible flow and with quite large amplitudes. This has been observed in actual practice and wind tunnel testings along with the fact that the fluttering membrane exhibits waves moving in the direction of the airstream. Thus an aeroelastician is confronted with the problem of high amplitude

travelling wave membrane flutter in incompressible flow. There seems to be very little literature available in this area. Motivated by this fact, a preliminary attempt has been made to analyse this problem in the present work. To account for the arbitrary ~~boundary conditions~~ boundaries and to treat the problem as realistically as possible, finite element method has been employed for the analysis.

1.2 Literature Survey

As stated earlier, very meagre literature is available on travelling wave flutter of membranes with flexible boundaries, in incompressible flow. However, the problem of panel flutter both in subsonic and supersonic flows has been investigated extensively during the past twenty years, both theoretically and experimentally. In the following, few investigations relevant to the present work will be reviewed.

The first recognition of panel flutter as an engineering problem was by Jordan (4) who indicated that a number of early German V-2 missile failures were supposed to be due to this instability. His investigations were based on unpublished war time research. He identified the fact that a flag flutters at quite low speeds forming travelling waves and so does a skin panel made of thin paper (membrane), if it is not too tightly streched. Contrary to the theoretical predictions he stated that a flag of fabric held in

a supersonic stream will no longer flutter but will stay stiff as a board. Thus he concluded that paper or fabric skins can flutter at quite low speeds whereas metal skins due to their higher modulus, require higher speeds, and if they flutter at all, do so with very small amplitude. At sufficiently high speeds, any disturbance that might arise is dissolved into smaller and smaller waves and the result is a skin that gives the appearance of being stable.

Noticing the analogy between the panel flutter and the classical problem of the generation of water waves by wind and flutter of flags and sails, Miles (5) carried out panel flutter analysis by studying the progressive waves in a plate immersed in a flow. He represented the transverse deflection by a travelling wave motion and solved the complex eigenvalue problem. Goland and Luke (6) treated the problem of a vibrating membrane in a supersonic stream by the method of Laplace transform. For pressure distribution they used the expression given by Miles (7) for an oscillating airfoil, and found that for the membrane, flutter cannot occur at high supersonic speeds. Hedgepeth (8) explained the qualitatively dissimilar behavior of plates and membranes at high Mach numbers. According to this analysis, plate panels flutter at high supersonic Mach numbers while membranes do not.

In reference (9) Fung formulated a two dimensional panel flutter problem in the form of an integral equation

and solved it numerically by the method of iteration and the method of matrix approximation. He also pointed out the difficulty in using the Galerkin method for a membrane since the existence of a real eigenvalue depends upon the convergence of the solution. Again Fung (10) suggested that for a realistic theory the panel flutter should be studied as a problem in nonlinear mechanics.

Dugundji et al. (11) investigated the subsonic aeroelastic stability of a two-dimensional panel resting on a continuous elastic foundation both theoretically and experimentally. They also observed a definite flutter of a travelling type. Instabilities were found to occur when the complex values of wave velocity (eigenvalue) possess negative imaginary parts. For a finite panel Galerkin type solution was obtained by assuming the modes satisfying the pinned end boundary condition. Hedgepeth et al. (12) analysed the dynamic stability of an infinitely long panel on equally spaced supports, having an airstream of arbitrary speed on one side and dead air on the other; using two-dimensional linearized compressible flow theory together with elementary beam theory. A travelling wave expression was assumed for the transverse deflections. The problem of finding the aerodynamic forces was reduced to the determination of the pressures acting on a stationary wavy wall, of shape given by the spatial periodicity of transverse deflections, having a flow of velocity

equal to (free stream velocity + wave velocity) above and a flow of velocity equal to wave velocity below the wall.

Taneda (13) investigated a classical problem of waving motion of a flag experimentally in a low turbulence wind tunnel. He observed that the flag flutters in various oscillation modes with a travelling wave motion at the trailing edge. Sunderarajan (14) studied the effect of a rigid boundary placed parallel to a long panel with finite width assuming a travelling wave expression for transverse deflection. The aerodynamic pressure was calculated using Fourier transform technique. He concluded that the effect of the rigid boundary is considerable in lowering the flutter speed when it is placed very close to the fluttering panel. In references (15), (16) and (17) the supersonic membrane flutter problem is considered as a special case of a panel with negligible flexural rigidity but having high inplane tension. Dowell (18) and Morino (19) studied the problem of nonlinear panel flutter. The nonlinearity due to the membrane forces was included in Von Karman's large deflection equations. Dowell applied Gelerkin method and the system of nonlinear ordinary differential equations in time was solved by numerical integration.

The method of analysis in the above investigations broadly consists of the following steps.

(i) Expand the structural deformation in a series of natural or atleast complete modes.

(ii) Determine the aerodynamic forces for the given modal deformations.

(iii) Using these in the equations of motion, apply Galerkin's method to arrive at a set of ordinary, nonlinear, integro-differential equation in time for the modal amplitudes.

(iv) Solve these equations by a numerical integration with respect to time.

In the literature there are many individual variations from investigator to investigator in the use of theories to get aerodynamic loading, in the representation of the panel deflection and deriving the equation of motion. As structures became more complicated with arbitrary boundaries, the conventional methods like Galerkin's and Rayleigh-Ritz proved incapable of yielding accurate solutions to them. Recently, therefore, few investigators (20,21,22,23,24) have attempted to use finite element techniques to solve flutter problems.

Kariappa et al. (21) analysed successfully a simply supported skew panel in supersonic flow through this approach. Aerodynamic influence coefficient matrices that are kinematically consistent with the stiffness and inertia matrices were derived using the principle of virtual work. The use

of assumed modes was avoided by solving directly the complex eigenvalue problems for studying the stability characteristics. A further application of finite elements was presented by Olson (22) in which he used two rectangular plate bending elements (12-parameter non-conforming model and the 16-parameter conforming one) and an 18-parameter conforming triangular element. He concluded that conforming rectangular element yielded higher accuracy and faster convergence than the non-conforming one. A further extension of work of (21) is presented in (23,24). In (24) Kariappa et al. considered the flutter problem of skew panels with inplane forces under yawed supersonic flow. The effect of mid plane forces was included using the concept of geometric stiffness matrix.

1.3 Object and Scope

Present work deals with the analysis of moderately large amplitude membrane flutter of travelling wave type in an incompressible flow using finite element technique. The analysis made is completely a general one and is valid for any set of kinematic boundary conditions. The main object of the present work is to provide a theoretical analysis for the aforementioned problem, which has been studied experimentally in the Dept. of Aero. Engg., I.I.T. Kanpur. The idea being to predict the results theoretically. A check on the analysis can be made and necessary modifications be incorporated if needed, by comparing these

theoretical results with those of experimental study. In the tests the rectangular convass cloth model was tested by fixing it at its four corners. These boundary conditions were chosen, because the flutter could occur only for these conditions within the available tunnel speed range. Therefore, in the present analysis also this set of boundary conditions is ~~are~~ considered.

Chapter 2 gives an account of experimental study of the problem. It includes the experimental set-up, instruments and procedure. Observations and inferences have been presented to act as a guideline for the theoretical analysis. Chapter 3 gives the structural idealization of the membrane by dividing it into 16 rectangular elements. The function is discretized using Hermite polynomials as the interpolation functions. Kinematically consistent aerodynamic matrix is derived through virtual work principle by representing the membrane with a sheet of point sources and using linearized small perturbation theory. In Chapter 4 the stiffness and mass matrices are derived using the principle of strain energy and virtual work concept. Nonlinearity due to high amplitudes of the fluttering membrane and the effect of inplane tension, are taken into account through the derivation of geometric stiffness matrix. Transformation matrices from local to global coordinates are derived in Chapter 5 and a method is given for assembling the aerodynamic, stiffness and mass matrices.

After accounting for the boundary conditions the complex eigenvalue problem is formulated. Chapter 6 indicates the method of solution. Appendices at the end gives the detailed calculations of stiffness and mass matrices and the transformation matrices.

CHAPTER 2

EXPERIMENTAL STUDY OF THE MEMBRANE FLUTTER PHENOMENON

2.1 General

As described in Section 1.1, a necessity was felt to study the phenomenon of membrane flutter. A theoretical analysis was therefore needed to predict this behaviour. To make this analysis more realistic, it was decided to have a physical picture of the flutter phenomenon, so that it could act as a guideline for the theoretical investigation. Simple experiments were therefore conducted using the tunnel available in the Dept. of Aero. Engg., I.I.T. Kanpur. The necessary apparatus was built by the author and Banta, who was interested in making very detailed parametric studies of the phenomenon (26).

2.2 Apparatus and Procedure

2.2.1 Wind Tunnel

The experiments were conducted in the low speed 3'x2', three dimensional closed circuit wind tunnel, available in the Department of Aeronautical Engineering, I.I.T. Kanpur.

The maximum speed of the tunnel was 42 metres per second. To observe the amplitude and shape of the fluttering membrane a grid work of 2 cms square was made on a sheet of

black paper and was pasted on the facing vertical wall of the 5 ft. long test section. This also provided the necessary black background for the model to take the photographs.

2.2.2 Design of Membrane Fixture

While designing the fixture, due considerations were given so that minimum alterations were required in the existing test section. The other factors considered were the ready installation and ease in fabrication of the fixture. With these considerations a very simple and multipurpose fixture was designed and is shown in Figure (2.1). It consisted of four adjustable, each 60 cms. long and 2 cms. in diameter, vertical mild steel rods threaded all along their length, with 25 cms. long flanges attached at their top. In the test section floor six holes,of 2 cms. dia. each,were drilled. The vertical supports could be fixed in any set of four holes corresponding to the required dimensions of the membrane. Additional extension strips of various sizes, as shown in Figure 2.4, were provided to accommodate any configuration any dimension and any type of boundary condition.

2.2.3 Test Model

For observation purposes a rectangular membrane model was prepared out of a 0.06 cms. thick convas$ cloth sheet.

In actual practice the requirements of edge conditions for the membrane are different in different applications. It

was possible to test the membrane with almost all possible type of edge conditions with fixture designed in Section (2.2.2). Trials were performed at the following sets of boundary conditions.

(i) All edges clamped.

(ii) Only leading edge and trailing edge clamped and sides free.

(iii) Leading edge clamped and trailing edge fixed with flexible mild steel wire, sides free.

(iv) Both leading edge and trailing edge fixed with flexible mild steel wire.

In all these cases the membrane was stable within the available speed range.

Then it was decided to further relax the boundary conditions by fixing it at its four corners only. In this case all the edges were stiffened by applying a thin coat of dope on them. For this set of flexible boundaries the flutter occured within the tunnel speed range. So, these conditions were retained for further observations.

2.2.4 Pressure Probe

It was planned to record the pressure distribution over the membrane during flutter with the idea of determining the pressure distribution in the neighbourhood and at instability. For this purpose a pressure probe was made,

which consisted of seven static and one total head tubes, covering the entire width of the membrane. These tubes were attached at the ends of two long brass tubes stemming from the top surface of the test section (as shown in Figure 2.2). By traversing that probe from leading edge to trailing edge, the pressure distribution on the complete membrane, both along stream and across stream could be recorded.

For this purpose a traversing arrangement, as shown in Figure 2.3, was devised. To fit this arrangement the existing top of the tunnel test section was replaced by a new one having two slits of one cm. width each and 45 cms. apart. To enable the traversing on either side of the membrane surface, while the tunnel was running, the probe was made in two parts. One contained 3 static tubes and the other had 4 static and one total head tube. Both parts could be engaged and disengaged as desired with the help of a 'C' clamp provided for the purpose, without stopping the tunnel.

2.2.5 Manometer

An inclined multitube manometer with distilled water as its working medium, was used to measure speed and pressure distribution. Tunnel static and total pressure connections were given to the manometer so that their difference gave the dynamic head inside the tunnel. Measuring the temperature of the airstream inside, with an alcohol thermometer, the air density corrections were made while calculating the

airspeed from the noted dynamic pressure.

The pressure probe tubes were also connected to the same manometer and from the manometer readings the pressure coefficient was plotted along and across the membrane length.

2.2.6 Stroboscope

The frequency of the fluttering membrane was obtained by using the strobotac. With this the oscillating membrane was made stationary and the mode shape, amplitude and the nature of the oscillations were observed by taking a photograph of the stationary membrane as shown in Figure 2.4.

2.3 Observations

2.3.1 Development of the Flutter Phenomenon

The membrane was fixed at its four corners on the fixture and the tunnel speed was raised gradually from zero onwards. The nature of the development of oscillations was noted at successive increments in speed. These observations are described in the following.

At very low speeds the membrane stayed in a slightly deflected shape with occasional gentle oscillations of small amplitude. As the speed was raised, these oscillations grew larger in amplitude and, at times, irregular sudden jerks were observed. At still higher speeds membrane took a shape forming a peak near the leading edge and a shallow and long dpression near the trailing edge. At the same speed they

interchanged their positions by occasional up and down movement. A slight further increase in the airspeed pushed the leading edge peak to the downstream side and this resulted in a quite regular motion of the membrane. In these regular oscillations, the peak formed at the leading edge, due to some flow disturbance, appeared to move towards the trailing edge. The whole phenomenon looked as if some small spherical caps were being conveyed from leading edge towards trailing edge through the membrane. These caps were the disturbances created at the upstream side, that were moving towards the downstream edge of the membrane. This was identified as the 'travelling wave flutter'. The stage at which this phenomenon occured was defined as the 'onset' of flutter.

Once the flutter occured, the strobotac was switched on and the strobotron lamp was focused on the oscillating membrane. In the beginning, the strobotron light was projected at its highest frequency. The frequency was then decreased gradually till the first single stationary image of the fluttering membrane was obtained. To differentiate betwee single and multiple images a coloured spot was marked on the membrane surface. The single image was observed when only one image of the spot was seen stationary. While making the membrane stationary the waves appeared moving against the stream, at the strobotac setting higher than the actual frequency. At a lower setting they appeared moving along the

stream. In between these two readings there was a setting at which the membrane just appeared to be stationary as shown in Figure 2.4. At this condition the mode shape consisted of generally 3 peaks and depression (in some cases there were 2 peaks also). This setting corresponded to the flutter frequency and the corresponding tunnel speed was the flutter speed.

2.3.2 Pressure Measurement

Knowing the flutter onset from the first run, the airspeed in the second run was kept to a value slightly less than the onset speed. The pressure distribution was measured at this speed. In the manometer, the pressure probe readings showed a decrease in pressure over the peak and a relative increase in pressure over the depression on both the surfaces. Next the airspeed was raised till the flutter speed was attained. Again the pressure distribution was measured at this stage. The pressure plots are shown in Figure 2.6.

Because of the unsteady oscillations, the readings in the manometer were also changing from instant to instant. At any instant the pressure plot was resembling very nearly the deflected shape of the membrane. As the membrane mode shape was changing, so did the pressure distribution. To record a time history of these unsteady pressure readings high speed film records were taken with a 16 mm. movie camera. But the development of the film could not be arranged in time.

So, only the mean manometer readings were taken and corresponding mean pressure distribution was plotted to get a rough idea of the aerodynamic pressure distribution over the fluttering membrane.

2.3.3 Inplane Tension Effects

Some observations were made to see the effect of inplane tension on flutter. For this the membrane was stretched arbitrarily in the beginning and then tested. In that case it was observed that the flutter speed was raised and the lateral deflections were also restricted. A relatively low amplitude travelling wave flutter was observed with higher flutter speed and frequency, as shown in Figure 2.5.

2.4 Inferences

From the observations made in Section (2.3) following inferences were drawn:

1. During instability, the membrane exhibited waves that travelled towards downstream side. Thus the membrane flutter phenomenon was of travelling wave type.

2. Edge conditions played an important role in the membrane flutter behaviour. The more the edges are restrained, the higher is the flutter speed.

3. In certain cases membrane was fluttering with moderately large amplitudes whereas in others, quite large amplitudes were noticed.

4. Inplane tension had a favourable effect in the flutter

CHAPTER 3

STRUCTURAL IDEALIZATION OF MEMBRANE AND DERIVATION OF AERODYNAMIC MATRIX

3.1 Finite Element Method

In any elastic continuum the solutions for both the static and dynamic problems, are in most cases very difficult if not impossible, because of infinite degrees of freedom. The concept of finite elements attempts to overcome this difficulty by approximating the real continuum to a finite degrees of freedom. In this case it is visualised as an assemblage of simple structural elements interconnected at a discrete number of nodal points at which some fictitious forces are supposed to act. The problem then reduces to the solution of a set of these simple elements, amenable to numerical analysis.

This concept of finite elements can briefly be summarized in the following manner:

(1) The continuum is divided by imaginary lines or surfaces into a number of finite elements. (Discretization of Region).

(2) The elements are assumed to be interconnected at a discrete number of nodal points situated on their boundaries. The displacements (or the forces) at these nodal points will be the basic unknown parameters of the problem.

(3) A function is chosen to define uniquely the state of displacement (or forces) within each finite element in terms of its nodal displacements. (Discretization of function)

(4) The displacement functions now define uniquely the state of strain within an element in terms of the nodal displacements. These strains, together with any initial strains and the elastic properties of the material will define the state of stress throughout the element and, hence, also on its boundaries.

(5) A system of forces concentrated at the nodes and equilibrating the boundary stresses and any distributed loads is determined, resulting in a stiffness matrix for the element.

(6) Knowing the stiffness properties of individual elements, the behaviour of the assembled structure can be studied through any well known technique of structural analysis.

Thus finite element analysis may be thought of as an assumed mode analysis in which the assumed modes, instead of having an uniform definition over the entire structure, have a different definition in each zone or subelement, producing a sort of discretised assumed mode. The local modes (usually polynomials) are assumed, for convenience, such that the undetermined coefficients correspond to physical degrees of freedom at the nodes of the element.

The finite element approximation essentially reduces to the problem of minimizing a 'functional' representing the total potential energy defined in terms of a finite number of nodal parameters and formulating a set of simultaneous equations. Among all the available techniques of structural analysis, finite element approach is considered to be the most powerful technique and is best suited to assemble the complex and realistic configurations from relatively simple element shapes.

3.2 Structural Idealization of Membrane

3.2.1 Discretization of Region

The degree of approximation achieved through the finite element method depends very much on the choice of element shape and of the form of the displacement function. The choice of element shape further depends on the nature of the problem. In vibration and flutter problems of panels the plate bending elements are used.

To get a real picture of the problem this choice was based on the experimental observations described in Chapter 2. These observations can be of a great help in selecting the shape of elements to approximate the exact deformed configuration of the membrane.

3.2.1.1 Choice of Element Shape

For initial discretization for arbitrary panel configurations, flat triangular and quadrilateral elements give

the best approximation. But in the case of regular configuration like a rectangular panel, the simple flat rectangular shape is the obvious choice.

For oscillations of moderately large amplitudes as shown in Figure (2.5) the deformation of the membrane remains within the reach of shallow shell theory. Thus while applying the incremental step approach, the behaviour of this continuously curved surface, formed after first step, can be adequately represented, during any subsequent step, by the behaviour of a surface built up of small flat elements. The only difference in that case will be that local coordinates for these flat elements will keep on changing from step to step.

For still larger deflections as shown in Figure (2.4) the shape of the membrane becomes more shell like and the above representation seems to be unsatisfactory for this case. Here the curved shell elements have to be considered in each step to approximate the deformed shape of the membrane.

3.2.1.2 Choice of Element Size

The investigators in the past have shown that in thin plate structures even a gridwork of 4 elements (2x2) gives reasonably good results. As the size of the element is decreased, the accuracy, of course, increases but the mathematics becomes quite involved. As observed in these Figures (2.4) and (2.5) the division of the membrane into 16 elements

forming a 4x4 mesh is expected to give good results.

3.2.1.3 Division of Membrane into Discrete Elements

In accordance with the considerations discussed in Sections (3.2.1.1) and (3.2.1.2), the rectangular membrane shown in Figure 3.1 is divided into 16 flat rectangular elements. Thus a relatively finer 4x4 gridwork is obtained as shown in Figure 3.2. The local co-ordinate axes for a typical element, as shown in Figure 3.3, are taken along the global co-ordinate axes. With this selection of co-ordinate axes the elemental characteristics obtained in the local co-ordinates are the same as in the global co-ordinate system. This helps in simplifying the assembly process.

3.2.2 Discretization of Function (Choice of Element Shape Function)

The state of deformation of the oscillating membrane can be described by the lateral field displacement w, which has to be expressed in terms of nodal displacements using the element shape functions. At any node 'i' of the element the following generalized displacements are considered.

Lateral displacements W_i and out of plane rotations i.e. $\partial w/\partial x$, $\partial w/\partial y$.

Suitable shape functions have to be determined now. Two types of shape functions are defined as follows:

(i) Conforming shape function: which ensures the complete continuity of displacement w and of slopes $\partial w/\partial x$, $\partial w/\partial y$ along

an interface between various elements.

(ii) Non-conforming shape functions: which preserve the continuity of w but violates the slope continuity between the elements, though not at the node where continuity is imposed.

In the solutions of first type the mathematical and computational difficulties often rise disproportionately fast. However, it is relatively simpler to obtain the solutions of second type.

Proceeding from the idea that the imposition of slope continuity at nodes must, in limit, lead to a complete slope continuity, several very successful elements have been developed (Zienkiewicz, Clough, Argyris etc.). Bazeley et al.(27) have established the superiority of non-conforming solutions over conforming ones for most of the static problems. To verify this superiority for the membrane flutter problem analyses of both kinds have to be made. In the present analysis, the non-conforming shape functions have been used.

By using the products of one-dimensional interpolation functions it has been observed that it is possible to generate displacement states having the property that displacements along an edge depend only on degrees of freedom common to that edge. This is all that is required for geometric compatibility between the elements. These interpolation

functionsselected here are the Hermite polynomials as used by Bogner et al.(28). Retaining the same notation, a Hermite polynomial $H^N_{K_i}(x)$ is a polynomial of order 2N+2 which gives when $x = x_i$

$$d^m H/dx^m = 1 \qquad m = k \quad \text{for} \quad k = 0 \text{ to } N$$

and $$d^m H/dx^m = 0 \qquad m \neq k$$

where N is the number of derivatives that the set can interpolate and x_j are the specific values of the argument x of the polynomial. They can be used to interpolate a function f(x) and its derivatives at the two points '0' and 'a', given the values f(0), f(a), f'(0) and f'(a), as follows:

$$f(x) = f(0)\, H^{(1)}_{01}(x) + f(a)\, H^{(1)}_{02}(x) + f'(0)\, H^{(1)}_{11}(x) + f'(a) H^{(1)}_{12}(x)$$

In the present case f(x) corresponds to w and f(0), f(a) etc. are the Nodal displacements W_i's etc. In general they are defined as

$$H^{(0)}_{0i}(x) = \frac{x-x_j}{x_i-x_j} \; ; \quad H^{(1)}_{0i}(x) = \left[1-2(x-x_i)\,\frac{dH^{(0)}_{0i}(x_i)}{dx}\right]\left[H^{(0)}_{0i}(x)\right]^2$$

$$H^{(1)}_{1i}(x) = (x-x_i)\left[H^{(0)}_{0i}(x)\right]^2 \ldots \text{ and so on.}$$

For the present case of flat rectangular element with sides a and b the polynomials required are defined as follows:

$$H^{(1)}_{01}(x) = \frac{1}{a^3}(2x^3-3ax^2+a^3) \; ; \; H^{(1)}_{01}(y) = \frac{1}{b^3}(2y^3-3by^2+b^3) \quad (3.1a)$$

$$H^{(1)}_{02}(x) = -\frac{1}{a^3}(2x^3-3ax^2) \; ; \; H^{(1)}_{02}(y) = -\frac{1}{b^3}(2y^3-3by^2) \quad (3.1b)$$

$$H^{(1)}_{11}(x) = \frac{1}{a^2}(x^3-2ax^2+a^2x) \; ; \; H^{(1)}_{11}(y) = \frac{1}{b^2}(y^3-2by^2+b^2y) \quad (3.1c)$$

$$H_{12}^{(1)}(x) = \frac{1}{a^2}(x^3-ax^2) \; ; \; H_{12}^{(1)}(y) = \frac{1}{b^2}(y^3-by^2) \qquad (3.1d)$$

With the help of these polynomials the following field displacement is generated.

Assuming a travelling wave expression, the transverse deflection is written as

$$w(x,y,t) = e^{i2\pi/\lambda\,(ct-X)} \sum_{i=1}^{2}\sum_{j=1}^{2} (H_{oi}^{(1)}(x)\, H_{oj}^{(1)}(y)\, w_{ij} + H_{1i}^{(1)}(x).$$

$$H_{oj}^{(1)}(y)\, w_{x_{ij}} + H_{oi}^{(1)}(x)\, H_{1j}^{(1)}(y)\, w_{y_{ij}}) \qquad (3.2)$$

where λ = wave length

c = wave velocity

X is the global x-coordinate indicating that the travelling wave phenomenon occurs in the entire assembled membrane and not in each discrete element separately.

The inplane displacements accompanying these lateral oscillations can be neglected, because their effect being of second order, this does not cause any substantial error. Where w_{ij} etc. are the values of w at the point $x = x_i$; $y = y_j$ i.e. $w_{ij} = w(x_i, y_j)$ etc. (Refer to Figure 3.3)

In the matrix notation Eqn. (3.2) is written as follows:

$$w(x,y,t) = e^{i\,\lambda^*(ct-X)} \{W\}^T \{f\} \qquad (3.3)$$

where λ^* is the wave number defined by $\lambda^* = 2\pi/\lambda$ (3.4)

$$\{w\}^T = [\, w_1 \;\; w_2 \;\; w_3 \;\; w_4 \;\; w_5 \;\; w_6 \;\; w_7 \;\; w_8 \;\; w_9 \;\; w_{10} \;\; w_{11} \;\; w_{12} \,] \tag{3.5a}$$

and

$$\{f\} = \begin{Bmatrix} H_{01}^{(1)}(x) \cdot H_{01}^{(1)}(y) \\ H_{11}^{(1)}(x) \cdot H_{01}^{(1)}(y) \\ H_{01}^{(1)}(x) \cdot H_{11}^{(1)}(y) \\ H_{02}^{(1)}(x) \cdot H_{01}^{(1)}(y) \\ H_{12}^{(1)}(x) \cdot H_{01}^{(1)}(y) \\ H_{02}^{(1)}(x) \cdot H_{11}^{(1)}(y) \\ H_{01}^{(1)}(x) \cdot H_{02}^{(1)}(y) \\ H_{11}^{(1)}(x) \cdot H_{02}^{(1)}(y) \\ H_{01}^{(1)}(x) \cdot H_{12}^{(1)}(y) \\ H_{02}^{(1)}(x) \cdot H_{02}^{(1)}(y) \\ H_{12}^{(1)}(x) \cdot H_{02}^{(1)}(y) \\ H_{02}^{(1)}(x) \cdot H_{12}^{(1)}(y) \end{Bmatrix} \tag{3.5b}$$

3.3 Derivation of Aerodynamic Matrix

3.3.1 Pressure Distribution on the Membrane Element No.1

The pressure distribution on an oscillating wing or airfoil submerged in unsteady compressible flow is obtained by solving the linearized partial differential equation in

disturbance velocity potential ϕ . (Refer to Bisplinghoff et.al (29).)

$$\nabla^2\phi - \frac{1}{a_\infty^2}\left[\frac{\partial^2\phi}{dt^2} + 2V\frac{\partial^2\phi}{\partial x\partial t} + V^2\frac{\partial^2\phi}{\partial x^2}\right] = 0 \qquad (3.6)$$

Subject to the linearized boundary conditions

$$\frac{\partial\phi}{\partial z} = \frac{\partial z_u}{\partial t} + V\frac{\partial z_u}{\partial x}\ ;\ \text{for } z = 0^+ \ (x,y) \text{ in } R_a \qquad (3.7)$$

$$\frac{\partial\phi}{\partial z} = \frac{\partial z_l}{\partial t} + V\frac{\partial z_l}{\partial x}\ ;\ \text{for } z = 0^- \ (x,y) \text{ in } R_a \qquad (3.8)$$

where Ra is the portion of the x,y plane covered by the projection of the planform. Equations (3.7) and (3.8) represent the exact specification of tangency of the flow to the surface. For incompressible flow, the speed of sound becomes relatively large and equation (3.6) reduces to the Laplace's equation

$$\nabla^2\phi = 0 \qquad (3.9)$$

This method has its foundation in the assumption of small disturbances. Quasi steady state assumptions are made which amounts to say that entire field of particle velocities depends only on the instantaneous motion of the submerged membrane, quite independently of the past history of that motion. This behaviour stems from the fact that the speed of sound is effectively infinite, so that any change of boundary conditions is propagated instantaneously to all the particles. Here a noncirculatory incompressible potential flow is considered, in view of the fact that it demonstrates the above

mentioned property and is easier to deal with.

Thus our problem now is to solve the partial differential equation (3.9) subject to the boundary conditions

$$\left.\frac{\partial \phi}{\partial z}\right|_{z=0^+} = \frac{\partial w}{\partial t} + V \frac{\partial w}{\partial x} \qquad \text{on } R_a \qquad (3.10a)$$

$$\left.\frac{\partial \phi}{\partial z}\right|_{z=0^-} = -\left(\frac{\partial w}{\partial t} + V \frac{\partial w}{\partial x}\right) \qquad (3.10b)$$

and $$\frac{\partial \phi}{\partial z} = 0 \qquad \text{off } R_a \qquad (3.10c)$$

where R_a is the region consisting of the membrane element placed in x y plane and w(x,y,t) is the transverse deflection of the membrane. The porosity effects are not considered here.

Familiarity with the elementary tools of fluid mechanics suggests that all these requirements are met by distributing over R_a, a sheet of those solutions of Laplace's equation known as point sources. A single concentrated source centred at $x = \xi$, $y = \eta$, $z = \zeta$ has the velocity potential

$$\phi(x,y,z) = \frac{-H}{4\pi\sqrt{(x-\xi)^2 + (y-\eta)^2 + (z-\zeta)^2}} \qquad (3.11)$$

Equation (3.11) describes motion with spherical symmetry around its centre, from which the source is readily shown to be emanating a bulk of liquid into the surrounding space equal to its strength H. A sheet of these, spread continuously over the surface R_a, having strength $H(\xi, \eta)$ per unit area

in the neighbourhood of the point $(\xi,\eta,0)$ possesses the disturbance potential

$$\phi(x,y,z) = -\frac{1}{4\pi}\int_{R_a}\int \frac{H(\xi,\eta)\,d\xi\,d\eta}{\sqrt{(x-\xi)^2+(y-\eta)^2+z^2}} \qquad (3.12)$$

Now to satisfy the boundary condition (3.10), we calculate

$$\frac{\partial\phi}{\partial z}\Big|_{z=0^+} = -\frac{1}{4\pi}\operatorname*{Lt}_{z\to 0^+}\frac{\partial}{\partial z}\int_{R_a}\int \frac{H(\xi,\eta)\,d\xi\,d\eta}{\sqrt{(x-\xi)^2+(y-\eta)^2+z^2}}$$

Taking the differentiation inside the integral sign, as limits of R_a do not depend on z, we get

$$\frac{\partial\phi}{\partial z}\Big|_{z=0^+} = \frac{1}{4\pi}\operatorname*{Lt}_{z\to 0^+} z\int_{R_a}\int \frac{H(\xi,\eta)\,d\xi\,d\eta}{\left[(x-\xi)^2+(y-\eta)^2+z^2\right]^{3/2}} \qquad (3.13)$$

As z assumes smaller positive values, the integral is caused to vanish by its multiplying factor, except in the vicinity of point $\xi = x, \eta = y$, where the integrand tends to infinity. This region is isolated with a small square of side 2ϵ, obtaining

$$\frac{\partial\phi}{\partial z}\Big|_{z=0^+} = \frac{1}{4\pi}\operatorname*{Lt}_{z\to 0^+}\int_{y-\epsilon}^{y+\epsilon}\int_{x-\epsilon}^{x+\epsilon} \frac{H(\xi,\eta)\,d\xi\,d\eta}{\left[(x-\xi)^2+(y-\eta)^2+z^2\right]^{3/2}} \qquad (3.14)$$

Being a continuous function, $H(\xi,\eta)$ over the entire square differs from its central value $H(x,y)$ by an amount of order ϵ. Hence, if we neglect these small variations and introduce temporary integration variables $\xi' = (x-\xi)$; $\eta' = (y-\eta)$ we get

$$\frac{\partial \phi}{\partial z}\Big|_{z=o^+} = \frac{H(x,y)}{4\pi} \; z \xrightarrow{Lt.} o^+ \int_{-\epsilon}^{\epsilon}\int_{-\epsilon}^{\epsilon} \frac{d\xi' \, d\eta'}{[\xi'^2 + \eta'^2 + z^2]^{3/2}}$$

Using the integral formulae,

$$\int \frac{dx}{(x^2 \pm a^2)^{3/2}} = \frac{\pm x}{a^2\sqrt{x^2 \pm a^2}}$$

and $$\int \frac{dx}{a' + c' x^2 \sqrt{a + cx^2}} = \frac{1}{a'}\sqrt{\frac{a'}{ac' - a'c}} \tan^{-1} x\sqrt{\frac{ac' - a'c}{a'(a + cx^2)}}$$

the above equation becomes

$$\frac{\partial \phi}{\partial z}\Big|_{z=o^+} = \frac{H(x,y)}{4\pi} \; z \xrightarrow{Lt.} o^+ \left[2\tan^{-1}\left(\frac{\epsilon^2}{z\sqrt{2\epsilon^2 + z^2}}\right) - 2\tan^{-1}\left(\frac{-\epsilon^2}{z\sqrt{2\epsilon^2 + z^2}}\right)\right] \tag{3.15}$$

Now z and ϵ should approach zero in such a way that the ratio ϵ/z becomes indefinitely large. To ensure that terms omitted in going from (3.14) to (3.15) are truly negligible, we have to make ϵ vanish in such a way that we don't get any non-zero contributions from the Region R_a outside the small square. This is possible when ϵ remains large compared to z. In that case the argument of inverse tangent approaches infinity because of z being a small quantity as compared to ϵ, the denominator has a strong tendency to approach zero, as both ϵ and z vanish. Thus limiting in this way, the inverse tangents approach $+\frac{\pi}{2}$ and $-\frac{\pi}{2}$.

$$\therefore \frac{\partial \phi}{\partial z}\Big|_{z=o^+} = \frac{1}{2} H(x,y) \tag{3.16}$$

Coming up to the source sheet from the lower side reverses the algebraic signs of the arguments of the inverse tangents in (3.15) thus leading to

$$\frac{\partial \phi}{\partial z}\Big|_{z=o^-} = -\frac{1}{2} H(x,y) \tag{3.17}$$

Therefore, it is seen that the source produce the symmetrical discontinuity specified by equations (3.10a) and (3.10b) which can both be satisfied by setting

$$H(x,y) = \frac{\partial \phi}{\partial z}\Big|_{z=o^+} - \frac{\partial \phi}{\partial z}\Big|_{z=o^-}$$

$$= 2\left(\frac{\partial w(x,y,t)}{\partial t} + V \frac{\partial w(x,y,t)}{\partial x}\right) \tag{3.18}$$

Substituting (3.18), in (3.12), we get

$$\phi(x,y,z) = -\frac{1}{2\pi} \int_o^a \int_o^b \frac{\frac{\partial w(\xi,\eta,t)}{\partial t} + V \frac{\partial w(\xi,\eta,t)}{\partial \xi}}{\sqrt{(x-\xi)^2+(y-\eta)^2+z^2}} \, d\xi \, d\eta \tag{3.19}$$

Pressure distribution is now calculated by using the unsteady linearized Bernoulli's equations

$$\Delta p = p_U - p_L = -2\rho \left[\frac{\partial \phi}{\partial t} + V \frac{\partial \phi}{\partial x}\right] \tag{3.20}$$

Differentiating (3.19) with respect to x and t and setting z=o we get

$$\Delta p = \frac{\rho}{\pi} \left(\frac{\partial}{\partial t} \int_o^a \int_o^b \frac{\frac{\partial w(\xi,\eta,t)}{\partial t} + V \frac{\partial w(\xi,\eta,t)}{\partial \xi}}{\sqrt{(x-\xi)^2+(y-\eta)^2}} \, d\xi \, d\eta \right.$$

$$\left. + V \frac{\partial}{\partial x} \int_o^a \int_o^b \frac{\frac{\partial w(\xi,\eta,t)}{\partial t} + V \frac{\partial w(\xi,\eta,t)}{\partial \xi}}{\sqrt{(x-\xi)^2+(y-\eta)^2}} \, d\xi \, d\eta \right) \tag{3.21}$$

Now for element no. 1 Figure (3.2) X = x and ∴ equation (3.3) takes the following form

$$w(x,y,t) = e^{i\,\lambda^*(ct-x)} \{W\}^T \{f\} \qquad (3.22)$$

The aerodynamic lift force acting on the small area dx dy (Figure 3.5) is

$$\Delta P = \Delta p\, dx\, dy \qquad (3.23)$$

Substituting for w from (3.22) in (3.21) and then calculating ΔP from (3.23), we obtain

$$\Delta P = \{W\}^T e^{(i2\pi/\lambda)ct} \frac{\rho}{\pi} \left(\left(\frac{i2\pi c}{\lambda}\right)^2 \{I_1(x,y)\} + \left(\frac{i2\pi c}{\lambda} V\right) \cdot \left(\{I_2(x,y)\} + \{I_3(x,y)\} \right) + V^2 \{I_4(x,y)\} \right) dx\,dy \qquad (3.24)$$

where the vector $\{I\}$'s are given as follows:

$$\{I_1(x,y)\} = \int_0^a \int_0^b \frac{\bar{e}^{\,i2\pi/\lambda} \{f\}}{\sqrt{(x-\xi)^2+(y-\eta)^2}}\, d\xi\, d\eta \qquad (3.25a)$$

$$\{I_2(x,y)\} = \int_0^a \int_0^b \frac{\bar{e}^{i\xi\lambda^*}(\partial f/\partial \xi) - i\lambda^* \{f\}}{\sqrt{(x-\xi)^2 + (y-\eta)^2}}\, d\xi\, d\eta \qquad (3.25b)$$

$$\{I_3(x,y)\} = \frac{\partial}{\partial x} \int_0^a \int_0^b \frac{e^{-i\xi\lambda^*} \{f\}}{\sqrt{(x-\xi)^2+(y-\eta)^2}}\, d\xi\, d\eta \qquad (3.25c)$$

$$\{I_4(x,y)\} = \frac{\partial}{\partial x} \int_0^a \int_0^b \frac{e^{-i\xi\lambda^*} (\partial f/\partial \xi - i\lambda^* \{f\})}{\sqrt{(x-\xi)^2 + (y-\eta)^2}}\, d\xi\, d\eta \qquad (3.25d)$$

3.3.2 Derivation of Aerodynamic Matrix:

To consider the effect of this aerodynamic force ΔP, the aerodynamic matrix is calculated as follows:

The virtual work of the aerodynamic force ΔP is

$$V_a = \int_0^a \int_0^b \tilde{w} \quad \Delta P^T \, dx \, dy \qquad (3.26)$$

where $\tilde{w}$ is the virtual displacement.

Now

$$\tilde{w} = \{\tilde{W}\}^T \{f\} \quad e^{i \lambda^*(ct-x)}$$

Substituting this $\tilde{w}$ and Eqn. (3.24) in Eqn. (3.26) with λ^* as $= 2\pi/\lambda$, we get

$$V_a = e^{i2 \lambda^* ct} \frac{\rho}{\pi} \int_0^a \int_0^b \{\tilde{W}\}^T \{f\} \quad e^{-i \lambda^* x} ((i \lambda^* c)^2 \{I_1\}^T + (i \lambda^* c V)(\{I_2\}^T + \{I_3\}^T) + V^2 \{I_4\}^T) \{W\} \, dx \, dy \qquad (3.27)$$

This can be written as

$$V_a = \{\tilde{W}\}^T [A_e] \{W\} \qquad (3.28)$$

where the aerodynamic matrix $[A_e]$ is given by

$$[A_e] = e^{i2 \lambda^* ct} \frac{\rho}{\pi} \int_0^a \int_0^b (-\lambda^{*2} c^2 e^{-i \lambda^* x} \{f\} \{I_1\}^T + i \lambda^* c V e^{-i \lambda^* x} (\{f\} \{I_2\}^T + \{f\} \{I_3\}^T) + V^2 e^{-i \lambda^* x} \{f\} \{I_4\}^T) \, dx \, dy \qquad (3.29)$$

This can further be written as

$$\left[A_e\right] = -\lambda^{*2} c^2 \left[A_{e_1}\right] + i \lambda^* c V \left[A_{e_2}\right] + V^2 \left[A_{e_3}\right] \qquad (3.30)$$

where

$$\left[A_{e_1}\right] = e^{i2 \lambda^* ct} \frac{\rho}{\pi} \int_0^a \int_0^b e^{-i \lambda^* x} \{f\} \{I_1\}^T dx\, dy \qquad (3.31a)$$

$$\left[A_{e_2}\right] = e^{i2 \lambda^* ct} \frac{\rho}{\pi} \int_0^a \int_0^b e^{-i \lambda^* x} \left(\{f\} \{I_2\}^T + \{f\} \{T_3\}^T \right) dx\, dy \qquad (3.31b)$$

$$\left[A_{e_3}\right] = e^{i2 \lambda^* ct} \frac{\rho}{\pi} \int_0^a \int_0^b e^{-i \lambda^* x} \{f\} \{I_4\}^T dx\, dy \qquad (3.31c)$$

Equation (3.30) gives the aerodynamic matrix for element no.1.

3.3.3 Aerodynamic Matrices for other Elements

The global streamwise co-ordinate is related to the other elements as follows:

For element nos. 1, 5, 9, 13 ; $X = x$

For element nos. 2, 6, 10, 14 ; $X = x+a$

For element nos. 3, 7, 11, 15 ; $X = x+2a$

For element nos. 4, 8, 12, 16 ; $X = x+3a$ (3.32)

The expression for w will be modified according to Eqn.(3.32) and so will the aerodynamic matrix be. The aerodynamic matrices for rest of the elements are related to that for the 1st element in the following manner:

$$
\begin{aligned}
[A_e]^5 &= [A_e]^9 = [A_e]^{13} = [A_e]^1 \\
[A_e]^2 &= [A_e]^6 = [A_e]^{10} = [A_e]^{14} = e^{-i2\lambda^*_a}[A_e]^1 \\
[A_e]^3 &= [A_e]^7 = [A_e]^{11} = [A_e]^{15} = e^{-i4\lambda^*_a}[A_e]^1 \\
[A_e]^4 &= [A_e]^8 = [A_e]^{12} = [A_e]^{16} = e^{-i6\lambda^*_a}[A_e]^1
\end{aligned}
\tag{3.33}
$$

where $[A_e]^i$ denotes the aerodynamic matrix for ith element.

CHAPTER 4

DERIVATION OF STIFFNESS AND MASS MATRICES

4.1 General

In the dynamic problem of elasticity, a structural system is in equilibrium under the action of internal forces namely elastic, damping and inertia forces and the external applied forces. In the present problem, we assume no damping. The aerodynamic influence co-efficient matrix representing the external loading has been derived in Chapter 3. To represent the elastic and inertia forces the stiffness and mass matrices will be derived in this chapter.

4.2 Derivation of Stiffness Matrix

In deriving the stiffness matrix, geometric non-linearity caused by the large deflection of the oscillating membrane, is considered. This is connected with the strain-displacement equations. Even if strains remain small in the conventional sense, rotation of the element adds nonlinear terms to the strain-displacement equation. A geometric stiffness matrix is derived through the use of incremental step procedure to take this nonlinearity into account.

In general the stiffness matrix can be derived using any of the following methods:

(i) Unit displacement or virtual work method,

(ii) Castigliano's first theorem,

(iii) Differential equation method.

(iv) Inversion of displacement force relationship.

In the present work Castigliano's first theorem is used in which the strain energy U is written in terms of nodal displacements $\{W\}$. Then by this theorem the stiffness co-efficient k_{ij} is obtained as

$$k_{ij} = \frac{\partial^2 U}{\partial W_i \, \partial W_j} \tag{4.1}$$

where $\{W\}$ is the column vector of elemental nodal displacements given by Eqn. (3.5a). The equation (4.1) is written in a more concise form as follows:

$$U = \frac{1}{2} \{W\}^T ([A]^T [B] [A]) \{W\} \tag{4.2}$$

The stiffness matrix $[k]$, whose elements are k_{ij}, is then given by the triple matrix product as

$$[k] = [A]^T [B] [A] \tag{4.3}$$

Now strain energy is written as

$$U = \frac{1}{2} \int_v \{\epsilon\}^T \{\sigma\} \, dv \tag{4.4}$$

where the stress and strain vectors are defined as

$$\{\sigma\} = \begin{Bmatrix} \sigma_x \\ \sigma_y \end{Bmatrix} \quad ; \quad \{\epsilon\} = \begin{Bmatrix} \epsilon_x \\ \epsilon_y \end{Bmatrix}$$

Assuming the material of membrane to be elastic, the constitutive law is written as

$$\begin{Bmatrix} \sigma_x \\ \sigma_y \end{Bmatrix} = \frac{E}{1-\nu^2} \begin{bmatrix} 1 & \nu \\ \nu & 1 \end{bmatrix} \begin{Bmatrix} \epsilon_x \\ \epsilon_y \end{Bmatrix} \tag{4.5}$$

where ν is the Poisson's ratio.

. . For element no. 1, Eqn. (4.4) now becomes

$$U = \frac{1}{2} \frac{Eh}{(1-\nu^2)} \int_0^a \int_0^b \{\epsilon\}^T \begin{bmatrix} 1 & \nu \\ \nu & 1 \end{bmatrix} \{\epsilon\} \, dx \, dy \quad (4.6a)$$

where h is the thickness of the membrane and is constant through - out.

$$\text{or} \quad U = \frac{Eh}{2(1-\nu^2)} \int_0^a \int_0^b (\epsilon_x^2 + \epsilon_y^2 + 2 \, \epsilon_x \, \epsilon_y) \, dx \, dy \quad (4.6b)$$

4.2.1 Incremental Step Analysis

As discussed by Martin (30), in this method, large deformations are divided into smaller steps such that during each increment of step the problem can be treated as a linear problem. The total strain in each step can then be expressed as

$$\{\epsilon\} = \{\epsilon^o\} + \{\epsilon^a\} \quad (4.7)$$

where $\{\epsilon^o\}$ is the initial strain and $\{\epsilon^a\}$ is the developed strain during the step. Introducing (4.7) in (4.6b), the strain energy becomes

$$U = \frac{1}{2} \frac{Eh}{(1-\nu^2)} \int_0^a \int_0^b \Big[(\epsilon_x^o)^2 + (\epsilon_y^o)^2 + 2\nu(\epsilon_x^o)(\epsilon_y^o) + (\epsilon_x^a)^2 + (\epsilon_y^a)^2 + 2\nu(\epsilon_x^a)(\epsilon_y^a) + 2(\epsilon_x^o)(\epsilon_x^a) + 2(\epsilon_y^o)(\epsilon_y^a) + 2\nu\big((\epsilon_x^a)(\epsilon_y^o) + (\epsilon_y^a)(\epsilon_x^o)\big)\Big] \, dx \, dy \quad (4.8)$$

This is further written as

$$U = U_o + U_1 + U_2 \quad (4.9a)$$

where

$$U_o = \frac{1}{2} \frac{Eh}{(1-\nu^2)} \int_o^a \int_o^b (\epsilon_x^{o2} + \epsilon_y^{o2} + 2\nu\, \epsilon_x^o\, \epsilon_y^o)\, dx\, dy \quad (4.9b)$$

$$U_1 = \frac{Eh}{(1-\nu^2)} \int_o^a \int_o^b \left[\epsilon_x^o\, \epsilon_x^a + \epsilon_y^o\, \epsilon_y^a + \nu(\epsilon_x^a\, \epsilon_y^o + \epsilon_y^a\, \epsilon_x^o)\right] dx\, dy \quad (4.9c)$$

and

$$U_2 = \frac{1}{2} \frac{Eh}{(1-\nu^2)} \int_o^a \int_o^b (\epsilon_x^{a2} + \epsilon_y^{a2} + 2\nu\, \epsilon_x^a\, \epsilon_y^a)\, dx\, dy \quad (4.9c)$$

The first term U_o is simply the strain energy present prior to imposition of the additional disturbance and hence does not contribute to the stiffness.

The second term U_1 depends on the initial stress and hence yields the new stiffness matrix $[k_g]$ which depends on the state existing in the element prior to the imposition of an additional disturbance. This $[k_g]$ is known as 'initial stress stiffness' or 'geometric' stiffness matrix.

The third term U_2 depends on the additional strain. This gives the elastic stiffness matrix which is composed of the conventional small deflection elastic stiffness $[k_o]$ and the 'large displacement' (or initial displacement) matrix $[k_1]$. $[k_1]$ is a function of nodal displacements. In the present case $[k_o]$ will not be present. $[k]$ will contain only $[k_g]$ and $[k_1]$.

The introduction of this large displacement matrix in the equilibrium equations requires 'numerical iterative

processes based on trial and error method, for solution. Because of dependence of aerodynamic loads on displacements and vice versa, this hit and trial method involves lot of complexities in numerical computations in a flutter equation, where already two unknowns, namely the airspeed and the frequency, are present in the iteration process.

Therefore, as a first step, to simplify the analysis yielding a numerically feasible solution, we take $[k_1] = 0$. Furthermore considering the deflections to be 'moderately large', we can derive the elastic and geometric stiffness matrices in one step only, thus introducing a simple approximation.

Due to the additional in plane extension of the middle surface caused by the lateral deflection w of the oscillating membrane, the additional strain-displacement relationship becomes

$$\epsilon_x^a = \frac{1}{2} \left(\frac{\partial w}{\partial x}\right)^2 \qquad (4.10a)$$

and

$$\epsilon_y^a = \frac{1}{2} \left(\frac{\partial w}{\partial y}\right)^2 \qquad (4.10b)$$

The additional strains present in Eqn. (4.10) represent the rotation of the element out of its implane position in the xy plane. As stated earlier, the inplane displacements and rotations accompanied with lateral displacements are not considered.

4.2.2 Derivation of $[k_g]$

From Eqn. (4.10) and Eqn. (4.9c) we get

$$U_1 = \frac{Eh}{(1-\nu^2)} \int_0^a \int_0^b \left[\frac{1}{2} \epsilon_x^o \left(\frac{\partial w}{\partial x}\right)^2 + \frac{1}{2} \epsilon_y^o \left(\frac{\partial w}{\partial y}\right)^2 + \frac{1}{2}\nu\left(\epsilon_y^o \left(\frac{\partial w}{\partial x}\right)^2 + \epsilon_x^o \left(\frac{\partial w}{\partial y}\right)^2\right)\right] dx\, dy$$

Noting that

$$\begin{Bmatrix} \sigma_x^o \\ \sigma_y^o \end{Bmatrix} = \frac{E}{1-\nu^2} \begin{bmatrix} 1 & \nu \\ \nu & 1 \end{bmatrix} \begin{Bmatrix} \epsilon_x^o \\ \epsilon_y^o \end{Bmatrix} \qquad (4.11)$$

The above equation is written as

$$U_1 = \frac{1}{2} h \int_0^a \int_0^b \left(\sigma_x^o \left(\frac{\partial w}{\partial x}\right)^2 + \sigma_y^o \left(\frac{\partial w}{\partial y}\right)^2\right) dx\, dy \qquad (4.12)$$

writing (4.12) in the following form,

$$U_1 = \frac{1}{2} \int_0^a \int_0^b \begin{bmatrix} \frac{\partial w}{\partial x} & \frac{\partial w}{\partial y} \end{bmatrix} \begin{bmatrix} T_x^o & o \\ o & T_y^o \end{bmatrix} \begin{Bmatrix} \frac{\partial w}{\partial x} \\ \frac{\partial w}{\partial y} \end{Bmatrix} dx\, dy \qquad (4.13)$$

where T_x^o and T_y^o are the inplane tensions in x and y directions respectively. (with $T_x^o = \sigma_x^o h$; $T_y^o = \sigma_y^o h$)

we have

$$U_1 = \frac{1}{2} \int_0^a \int_0^b \{W\}^T [G]^T \begin{bmatrix} T_x^o & o \\ o & T_y^o \end{bmatrix} [G] \{W\}\, dx\, dy$$

$$= \frac{1}{2} \{W\}^T \left(\int_0^a \int_0^b [G]^T \begin{bmatrix} T^o & o \\ o & T_y^o \end{bmatrix} [G]\, dx\, dy \right) \{W\}$$

Comparing this with Eqn. (4.2), we have

$$U_1 = \frac{1}{2} \{W\}^T [k_g] \{W\} \qquad (4.14)$$

where

$$[k_g] = \int_0^a \int_0^b [G]^T \begin{bmatrix} T_x^o & \\ & T_y^o \end{bmatrix} [G]\, dx\, dy \qquad (4.15)$$

and

$[G]$ is defined as follows (referring to Eqns.(3.3-3.5) for element no.1

$$[G] = \begin{bmatrix} \frac{\partial}{\partial x} \{f\}^T & e^{i\lambda^*(ct-x)} \\ \frac{\partial}{\partial y} \{f\}^T & e^{i\lambda^*(ct-x)} \end{bmatrix} \qquad (4.16)$$

A term by term integration of Eqn. (4.15) yields the geometric matrix $[k_g]$.

4.2.3 Derivation of $[k_E]$

Now third term in the energy expression (4.9d) becomes

$$U_2 = \frac{Eh}{2(1-\nu^2)} \int_0^a \int_0^b \left(\frac{1}{4}\left(\frac{\partial w}{\partial x}\right)^4 + \frac{1}{4}\left(\frac{\partial w}{\partial y}\right)^4 + \frac{1}{2}\nu\left(\frac{\partial w}{\partial x}\right)^2 \left(\frac{\partial w}{\partial y}\right)^2\right) dx\, dy \qquad (4.17)$$

Here, because of cubic and fourth order terms U_2 gives the stiffness matrix as a function of displacements i.e. $[k_1]$, This may be retained or neglected according to the needs of the problem. Here it has not been ~~not~~ taken because of the difficultics mentioned earlier. So the stiffness matrix $[k]$ for the element will contain $[k_g]$ only. Thus for element no. 1,

$$[k] = [k_g] \qquad (4.18)$$

which is a 12x12 symmetric and complex matrix. The elements

4.2.4 Stiffness Matrix for Other Elements

Using Eqn. (3.32), the stiffness matrices for other elements are written as follows:

$$
\begin{aligned}
[k]^5 &= [k]^9 = [k]^{13} = [k]^1 \quad \text{given by Eqn. (4.18)} \\
[k]^2 &= [k]^6 = [k]^{10} = [k]^{14} = e^{-i2\,\lambda^* a}\,[k]^1 \\
[k]^3 &= [k]^7 = [k]^{11} = [k]^{15} = e^{-i4\,\lambda^* a}\,[k]^1 \\
[k]^4 &= [k]^8 = [k]^{12} = [k]^{16} = e^{-i6\,\lambda^* a}\,[k]^1
\end{aligned}
\qquad (4.19)
$$

4.3 Derivation of Mass Matrix

A straight-forward application of virtual work concept gives the mass matrix for element no. 1 as follows:

$$
[m] = \rho_m\, h\, e^{i2\,\lambda^* ct} \int_0^a \int_0^b e^{-i2\,\lambda^* x} \{f\}\{f\}^T \, dx\, dy \qquad (4.20)
$$

where ρ_m is the density of membrane material. It is a symmetric complex matrix whose elements are given in Appendix A.

4.3.1 Mass Matrix for Other Elements:

$$
\begin{aligned}
[m]^5 &= [m]^9 = [m]^{13} = [m]^1 \quad \text{given by Eqn. (4.20)} \\
[m]^2 &= [m]^6 = [m]^{10} = [m]^{14} = e^{-i2\,\lambda^* a}\,[m]^1 \\
[m]^3 &= [m]^7 = [m]^{11} = [m]^{15} = e^{-i4\,\lambda^* a}\,[m] \\
[m]^4 &= [m]^8 = [m]^{12} = [m]^{16} = e^{-i6\,\lambda^* a}\,[m]^T
\end{aligned}
\qquad (4.21)
$$

CHAPTER 5

ASSEMBLY OF ELEMENTS AND FORMULATION OF EIGENVALUE PROBLEM

5.1 General

Having derived the elemental aerodynamic, stiffness and mass matrices, we can put them together to yield the equilibrium equation for an element as

$$\left[k - \lambda^{*2} c^2 m - \lambda^{*2} c^2 A_{e_1} + i \lambda^* V c A_{e_2} + V^2 A_{e_3}\right] \{W\} = \{F\} \quad (5.1)$$

where $\{F\}$ is a column vector of generalized forces corresponding to the generalized co-ordinates $\{W\}$. The square matrix of Eqn. (5.1) represents the generalized 'aerodynamic stiffness matrix' for the element.

Now to obtain a complete solution the two conditions of

(i) displacement compatibility, and

(ii) equilibrium

have to be satisfied throughout.

The first condition is satisfied by listing a system of nodal displacements $\{W^*\}$ for the whole structure in which all the elements participate. Next the condition of overall equilibrium within an element is satisfied by Eqn. (5.1). All that is necessary to satisfy the second condition is to establish equilibrium conditions at the nodes of the structure.

This is accomplished by the assemblage of all the elements in which the equilibrium condition of a particular node is satisfied by equating, the sum of the generalized forces contributed by all the elements meeting at that very node, to zero. Thus on assembling the elements by equating the corresponding generalized co-ordinates at the global nodal points, a 'master aerodynamic stiffness matrix' is obtained.

In essence the assemblage of a structure requires the following steps:

1. Transformation of the elemental properties from their local co-ordinates to global ones.

2. Establishment of the transformation matrices $[a]$ relating the elemental nodal points to the global nodes as

$$\{W\} = [a] \{W^*\} \qquad (5.2)$$

3. Calculation of the characteristics of the structure. This is done by assembling according to the congruent matrix transformation e.g. for aerodynamic matrices we have

$$[A] = [a]^T [A_e] [a] \qquad (5.3)$$

Once the assembly is over the final eigenvalue problem is formulated on applying the homogeneous kinematic boundary conditions by striking out the appropriate rows and columns.

In the local co-ordinate system chosen in the present case where the elements are rectangular, the elemental

properties in the local and global co-ordinates system are identical. The first step, therefore, need not be carried out here. So, we directly move on to the second aspect of assembly process in the following section.

5.2 Establishment of [a] Matrices

In the complete membrane we have 16 elements with 25 global nodes as numbered in Figure (3.2). At 'i'th global node the generalized displacements are defined as follows:

$$\begin{aligned} W_i &= \text{displacement in Z-direction} \\ \theta_i &= \text{rotation about Y-axis i.e. } \frac{\partial w}{\partial x} \\ \phi_i &= \text{rotation about X-axis i.e. } \frac{\partial w}{\partial y} \end{aligned} \qquad (5.4)$$

and are shown in Figure 5.1. i takes the value from 1 to 25. Thus the (75x1) column vector of generalized displacements in global set is defined as

$$\{W^*\} = \begin{Bmatrix} W_1 \\ \theta_1 \\ \phi_1 \\ \vdots \\ W_{25} \\ \theta_{25} \\ \phi_{25} \end{Bmatrix} \qquad (5.5)$$

Similarly for a discrete element the four nodes are numbered as shown in Figure (3.3), alongwith the representation of the 3 generalized displacements at each node. The 12x1 vector

$\{W\}$ for this element is defined as

$$\{W\} = \begin{Bmatrix} W_1 \\ W_2 \\ \vdots \\ W_{12} \end{Bmatrix} \qquad (3.5a)$$

To relate $\{W\}$ to $\{W^*\}$, we derive the transformation matrix $[a_n]$ for each element.

Then for nth element

$$\{W\} = [a_n] \{W^*\} \quad (n = 1,\ldots 16) \qquad (5.6)$$

For element no. 1. $[a_1]$ is given as

$$[a_1] = \begin{bmatrix} 1 & & & \\ 01 & & & \\ 001 & & & \\ 0001 & & & \\ 00001 & & & \\ 000001 & & & \\ & 0_{15} & & \\ & & 1 & \\ & & 01 & \\ & & 001 & \\ & & 0001 & \\ & & 00001 & \\ & & 000001 & 0_{54} \end{bmatrix}$$

Where 0_{15} indicates a row containing 15 columns of zeroes and same is meant by 0_{54}. The transformation matrices for other elements (i.e. from $[a_2]$ to $[a_{16}]$) are given in Appendix B.

5.3 Assembly of the Elements

Knowing the transformation matrices for each element, the assembly for a particular characteristic (viz. Aerodynamic, stiffness, mass) is done according to the equation (5.3) as follows:

$$[K] = \sum_{n=1}^{16} [K_n] = \sum_{n=1}^{16} a_n^T k_n a_n \qquad (5.8)$$

The stiffness matrix [K] thus obtained represents the stiffness for the entire membrane.

As is seen from Eqn. (5.7), the matrices a_n's are very sparsely populated containing only unity as the non-zero elements. So, while computing the component matrices K_n's, to store these a_n's as such will be a waste of computer space as well as of computing time. To avoid this we may ignore all zeroes in the specification of the matrix a_n and merely indicate the position of 'unit' elements by specifying its row number i and column number j in the memory location. A typical K_n (in Eqn. 5.8) is calculated according to the flow diagram, shown in Fig. 5.2, suggested by Argyris (31).

The first step involves the operation $k_n a_n$. For a specific instruction (i, j) of an unit element this requires the transfer of the ith element of k_n to the jth column of the space provided for $k_n a_n$. In the second step we pre-multiply $k_n a_n$ with the transpose of a_n. There follows for the same unit element in question, a transfer of the ith row of $k_n a_n$ to the

jth row and the element is stored in the store allocation cleared for K. This process is repeated for n = 1 to 16 and the elements of K_n's are stored in their respective places. In the assembled [K] matrix a particular element K_{ij} will be obtained by adding all the elements in ith row and jth column of the store allocation contributed by all K_n's. In this way the full 75x75 [K] matrix is calculated. In a similar manner the aerodynamic and mass matrices are assembled. To achieve this a general assembly scheme is shown in Figure 5.4.

5.4 Formulation of Eigenvalue Problem

While setting up the $[a_n]$ matrices and during the assembly, the membrane is considered to be in a free-free state in space. For this state, sections 5.2 and 5.3 enable us to write the 75x75 master aerodynamic stiffness matrix as follows:

$$\left[K - \lambda^{*2} c^2 M - \lambda^{*2} c^2 A_1 + i \lambda^* c V A_2 + V^2 A_3\right] \tag{5.9}$$

In actual engineering applications such a free-free state of membrane never exists. It has to be supported with some structure in some manner to serve any useful purpose. The support conditions depend on the needs of the problem. However, the master aerodynamic stiffness matrix can be obtained for any support conditions from Eqn. (5.9) by simply omitting the appropriate rows and columns. As stated before, the object of this formulation is to give a theoretical analysis for membrane

flutter, which has been studied experimentally.

With this view, in this analysis the same configuration and boundary conditions are incorporated which were existing in the wind tunnel testings. In these experiments the support conditions had to be chosen as those of fixing the membrane at four of its corners (shown in Figure 5.3) because only then it became possible for the flutter to occur within the available tunnel speed range. These conditions correspond to zero displacements and rotations at the four nodes namely nos. 1, 5, 21 and 25. So, the master aerodynamic stiffness matrix for this set of boundary conditions, is obtained by striking rows and columns number 1, 2, 3, 13, 14, 15, 61, 62, 63, 72, 73, 74 in the matrix of Eqn. (5.9). The 63x63 matrix of Eqn. (5.9) is rewritten as

$$\left[K - \lambda^{*2} c^2 (A_1 + M) + i \lambda^{*} c V A_2 + V^2 A_3\right]$$

$$\text{Let } (A_1 + M) = M_A$$

Then above matrix becomes

$$\left[K - \lambda^{*2} c^2 M_A + i \lambda^{*} c V A_2 + V^2 A_3\right] \qquad (5.10)$$

Generally the aerodynamic damping matrix A_2 is neglected, as its contribution is relatively small. But in case it has to be retained then we will have to assume the possibility that this matrix $[A_2]$ differs from $[M_A]$ just by a scalar multiplier so that we can write

$$A_2 = p M_A \qquad (5.11)$$

With this we get the following equilibrium equation

$$\underset{63x63}{\left[K - \left(\lambda^{*2} c^2 - ip\lambda^* c V\right) M_A + V^2 A_3\right]} \underset{63x1}{\left\{W^*\right\}} = 0 \quad (5.12)$$

This can be further written as

$$\left[M_A\right]^{-1} \left[K + V^2 A_3\right] \left\{W^*\right\} = \left(\lambda^{*2} c^2 - ip \lambda^* c V\right) \left\{W^*\right\} \quad (5.13)$$

Equation (5.13) represents the conventional eigenvalue problem with $\left(\lambda^{*2} c^2 - ip \lambda^* c V\right)$ as the couplex eigenvalue.

CHAPTER 6

METHOD OF SOLUTION AND CONCLUDING REMARKS

6.1 Method of Solution

The dynamic equations under the influence of stiffness, inertia and aerodynamic forces have been reduced to the conventional form of eigenvalue problem in Section 5.4. Rewriting equation (5.13) we have

$$[B] \{w^*\} = \bar{\mu} \{w^*\} \qquad (6.1)$$

where

$$[B] = [M_A]^{-1} [K + V^2 A_3] \qquad (6.2a)$$

and $$\bar{\mu} = (\omega^2 - ip V \omega) \qquad (6.2b)$$

with ω as the angular frequency which is related to the wave velocity c through $\omega = \lambda^* c$. (6.2c)

The numerical analysis of the system (6.1) involve following steps.

1. Computation of elemental characteristic matrices:

The aerodynamic matrices can be evaluated after performing the necessary numerical integrations, for the desired panel dimensions 'a' and 'b'. The stiffness and mass matrices are functions of a, b and λ^*. The value of the wave number λ^* depends on the choice of wave length. In the wind tunnel tests, the wave length for a given membrane is easily observed. If this information is not available, the computation should

be started with an assumed wave mode. This then can be expressed as a fraction of the streamwise dimension of the membrane under test. Thus knowing the wave length corresponding to the desired panel dimensions 'a' and 'b', the wave number λ^* $(= \frac{2\pi}{\lambda})$ is known. By inserting the corresponding values of these parameters in the expressions of the aerodynamic, stiffness and mass matrices, their numerical values are determined.

2. Assembly of $[A_0]$, $[k]$ and $[M]$ and determination of $[M_A]$ and $[K+V^2 A_3]$:

The elemental matrices (k, A_e and m) obtained in step one are now assembled by the method indicated in Section (5.3). Then the simple addition of $[A_1]$ and $[M]$ gives $[M_A]$ and that of $[K]$ and V^2 $[A_3]$ gives $[K+V^2 A_3]$.

3. Evaluation of matrix $[B]$:

Matrix $[B]$ is obtained by inverting the matrix $[M_A]$ evaluated in step two and then postmultiplying this inverted matrix by $[K + V^2 A_3]$.

4. Solution for the eigenvalues of $[B]$:

The airspeed V is the only unknown contained in the complex matrix $[B]$. So, once this is assumed, $[B]$ is known completely. Then its complex eigenvalues can be determined by the standard subroutines available.

Flutter criterion:

The eigenvalue, $\bar{\mu}$, is a function of V and ω. The complex values of $\bar{\mu}$ corresponding to a known V, in general, gives a complex value of frequency. Let the complex eigenvalue and frequency be represented as

$$\bar{\mu} = \mu_R + i\ \mu_I \qquad (6.3a)$$

and $$\omega = \omega_R + i\omega_I \text{ respectively} \qquad (6.3b)$$

The real part of the frequency (ω_R) represents the oscillations while the imaginary part (ω_I) indicates the amplitude variations. The condition of instability depends only on ω_I. Whether ω_R is negative or positive, the wave still remains a combination of sine and cosine waves. When ω_I is positive the amplitude factor becomes $e^{-\omega_I t}$, thus the amplitude of the motion will decrease with increasing time. When ω_I is negative, the opposite is true.

If ω_I is positive at V_1 and negative at V_2 ($V_2 > V_1$), then there exists at least one value of V between V_1 and V_2, at which ω_I vanishes. At this speed ω is real, corresponding physically to a simple harmonic motion. Such a speed will separate the speed range in its neighborhood into two regions, in one of which $\omega_I > 0$ where the motion is damped and stable; in the other $\omega_I < 0$ where the amplitude increases with time and the motion is unstable. This speed at which $\omega_I = 0$, is called the 'critical speed'.

So far as ω_R is concerned, two cases are possible at the critical speed: Either ω_R vanishes, or it does not vanish. If $\omega_R = 0$, then the displacements are independent of time, but the structure has lost its power to recover its original form when disturbed. The panel is said to be in critical divergent condition. If $\omega_R \neq 0$, the motion is harmonic with an indefinite amplitude. It is said to be in the critical flutter condition. Hence,

$$\omega_I = 0, \quad \omega_R = 0 \quad \text{implies divergence}$$
$$\omega_I = 0, \quad \omega_R \neq 0 \quad \text{implies flutter.}$$

In both cases the aeroelastic system may be said to be neutrally stable.

From the available experiments, it looks as though ω_I has a very high positive value initially. As the speed is raised gradually, it keeps on decreasing till the onset speed is reached, where it becomes zero. At a slightly higher speed oscillations become divergent and it seems ω_I becomes negative. As the phenomenon of divergence was not observed, it is felt therefore that ω_R has a non-zero value at the critical speed and the instability is recognised as the flutter.

Now using Eqn. (6.3) the Eqn. (6.2b) is rewritten as

$$\mu_R + i\,\mu_I = (\omega_R + i\omega_I)^2 - ip\,V(\omega_R + i\omega_I) \quad (6.4)$$

Applying the above flutter criterion, we have at $V = V_{cr}$ $\omega_I = 0$. Thus Eqn. (6.4) is reduced to

$$\mu_R + i\,\mu_I = \omega_R^2 - i\,p\,V_{cr}\,\omega_R \qquad (6.5)$$

Equating the real and imaginary parts, we get

$$\omega_R = (\mu_R)^{1/2} \qquad (6.6)$$

and

$$\mu_I = -p\,V_{cr}\,(\mu_R)^{1/2} \qquad (6.7)$$

Eqn. (6.7) gives the relation between the real and imaginary parts of the eigenvalue $\bar{\mu}$ at the critical condition.

The values of airspeed V is now gradually increased and the corresponding (lowest) eigenvalue is found. The process is continued till the eigenvalue obtained is such that it satisfies the flutter criterion (6.7). The airspeed (V_{cr}) and the frequency ($\omega_{cr} = (\mu_R)^{1/2}$) corresponding to this condition give the flutter speed and the flutter frequency respectively. If the aerodynamic damping is neglected, then Eqn. (6.2b) reduces to

$$\bar{\mu} = \omega^2 \qquad (6.8)$$

and the corresponding flutter criterion becomes

$$(\mu_R)^{1/2} = (\omega_R)^{1/2} \qquad (6.9)$$

and

$$\mu_I = 0 \qquad (6.10)$$

Hence here we will seek for the existence of real eigenvalue for the flutter to occur.

The method of solution described above in steps 1-4 can be represented by a typical flow chart as shown below.

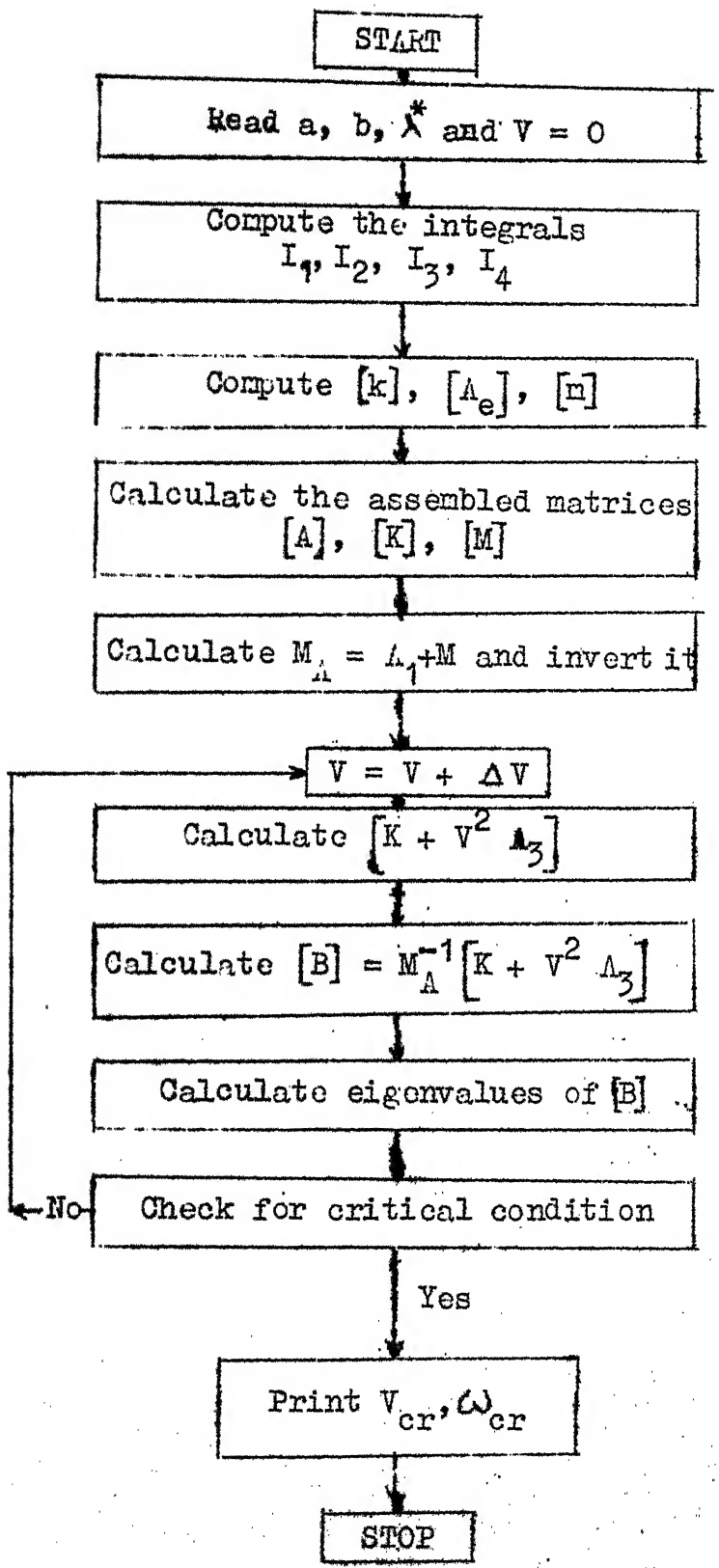

Flow chart for flutter solution.

6.2 Concluding Remarks

An analytical formulation for moderately large amplitude travelling wave membrane flutter in incompressible flow has been presented using finite element technique. The flow has been assumed to take place on both upper and lower surfaces of the membrane having flexible boundaries.

Unfortunately the aforementioned problem is of considerable complexity because of high order complex matrices encountered in the finite element method, structural nonlinearities and complicated aerodynamic expressions. The numerical evaluation of the integrations involved in the establishment of aerodynamic matrices and the computation of eigenvalues of the complex matrix is undoubtedly a difficult and time consuming task. In the present thesis, only the analytical formulation could be dealt with. Therefore, the investigation is by no means a complete one without the numerical analysis. However, in the formulation, every possible attempt has been made to present it in a form which is readily adaptable to computer programming. This helps in reducing the time required during the preliminary adjustments of the computer programming. The formulation presented is made general as far as possible to account for any set of boundary conditions, for a rectangular membrane. The specific boundary conditions chosen correspond to fixing the membrane at its four corners, as this is the situation existing in the experimental study of the

problem. This typical configuration cannot be analysed by any assumed mode solution, as no simple function is able to satisfy these boundary conditions. This reveals the necessity of finite element method because of its capability to treat such problems.

The membrane has been divided into 16 rectangular elements forming a 4x4 gridwork. A 12 parameter non-conforming model has been used. Small perturbation theory for non-circulatory incompressible flow has been employed to give the aerodynamic forces. The nonlinearity caused by the large deflections has been taken care of by deriving the geometric stiffness matrix. The aerodynamic matrix involves the integrations which have to be evaluated numerically. The elements for stiffness and mass matrices have been found by exact integrations. Their numerical values can be obtained on direct substitution of the panel dimensions and wave number.

The effect of inplane tension, size, aspect ratio and material density, on flutter behaviour can be readily studied by varying the appropriate parameters without altering the entire formulation.

6.3 Further Scope

To complete the investigation the first obvious task will be to find the numerical solutions for the present formulation. Once the results are obtained they can be compared with

the experimental results and the necessary improvements in the analysis can be done, if needed.

However, the following extensions are worth carrying out to strengthen the analysis:-

(1) Incorporating the conforming model in the analysis.

(2) Increasing the number of elements.

(3) Applying the incremental step approach with more number of steps by reducing the step size.

(4) Considering the large displacement matrix $[K_L]$.

(5) Considering the curved shell elements during process (2).

(6) Modifying the aerodynamic theory to study the flutter behaviour of the membrane placed at an angle of attack, and at higher speeds.

Any other configuration can be analysed by using the triangular elements, along the same lines as discussed in the present work.

REFERENCES

1. Nielsen, J.N., Theory of Flexible Aerodynamic Surfaces, J. App. Mech., pp 435-442, Sept.1963.

2. Thwaites, B., The Aerodynamic Theory of Sails, Part I - Two Dimensional Sailes, Proc. Royal Society, Series A, Vol. 261, pp 402-422, 1961.

3. Rogallo, F.M.; Lowry, J.G.; Croom, D.R. and Taylor, R.T., Preliminary Investigation of a Paraglider, NASA TN D - 443, Aug. 1960.

4. Jordan, P.F., Physical Nature of Panel Flutter, Aero. Digest, pp 34-38, Feb. 1956.

5. Miles, J.W., On the Aerodynamic Instability of Thin Panels, J. Aero. Sci. 23, 8, 771-780, Aug. 1956.

6. Goland, M. and Luke, Y.L., An Exact Solution for Two-Dimensional Linear Panel Flutter at Supersonic Speeds, J. Aero. Sci., 21, pp 275-276, Apr. 1954.

7. Miles, J.W., The Aerodynamic Forces on the Oscillating Airfoil at Supersonic Speeds, J. Aero.Sci., June 1947.

8. Hedgepeth, J.M., On the Flutter of Panels at High Mach No's., J. Aero. Sci., June 1956.

9. Fung, Y.C., On Two-Dimensional Panel Flutter, J. Aero. Sci., 25,3, March 1958.

10. Fung, Y.C., Some Recent Contributions to Panel Flutter Research, AIAA J., 1,4, 898-909, Apr. 1963.

11. Dugundji, J.; Dowell, E. and Perkin, B., Subsonic Flutter of Panels on Continuous Elastic Foundations, AIAA J., 1,5, 1146-1154, May 1963.

12. Hedgepeth, J.M.; Budiansky, B. and Leonard, R.W., Analysis of Flutter in Compressible Flow of a Panel on Many Supports, J.Aero.Sci., 21, 475-486, July 1954.

13. Taneda, S., Waving Motions of Flags, J. Physical Society of Japan, 24,2, 392-401, Feb. 1968.

27. Bazeley, G.P.; Cheung, Y.K.; Irons, B.M. and Zienkiewicz, O.C., Triangular Elements in Plate Bending - Conforming and Non-Conforming Solutions, 547-576, Proc. of Conference on Matrix Methods in Structural Mechanics, Wright-Patterson Air Force Base, Dayton Ohio, Dec. 1965.

28. Bogner, F.K.; Fox, R.L. and Schmit Jr., L.A., The Generation of Interelement Compatible Stiffness and Mass Matrices by the Use of Interpolation Formulas, 397-443, Proc. of Conference on Matrix Methods in Structural Mechanics, Wright-Patterson Air Force Base, Dayton Ohio, Dec. 1965.

29. Bisplinghoff, R.L.; Ashley, H. and Halfman, R.L., Aeroelasticity, Addison-Wesley Publishing Company, 1957.

30. Martin, H.C., On the Derivation of Stiffness Matrices for the Analysis of Large Deflection and Stability Problems, 697-716, Proc. of Conference on Matrix Methods in Structural Mechanics, Wright Patterson Air Force Base, Dayton Ohio, Dec. 1965.

31. Argyris, J.H., Recent Advances in Matrix Methods of Structural Analysis, Proc. in Aeronautical Sciences, Vol. 4, Pergamon Press, New York, 1964.

32. Durvasula, S. and Chopra, I., Report No. AE 2435, I.I.Sc., Bangalore, Apr. 1969.

33. Zienkiewicz, O.C., The Finite Element Method in Engineering Science, Mcgraw-Hill, London, 1971.

34. Fung, Y.C., Introduction to the Theory of Aeroelasticity, N.Y., John Wiley, 1955.

35. Novozhilov, V.V., Foundations of the Nonlinear Theory of Elasticity, Graylock Press, New York, 1953.

APPENDIX 'A'

ELEMENTS OF STIFFNESS AND MASS MATRICES

On performing the detailed integrations and calculations, the elements of stiffness and mass matrices derived in Chapter 4, will be presented here.

Stiffness Matrix:

Equation (4.16) gives the stiffness matrix as follows:

$$[k] = \int_0^a \int_0^b [G]^T \begin{bmatrix} T_x & 0 \\ 0 & T_y \end{bmatrix} [G] \, dx \, dy$$

where $[G]$ is given by equation (3.17).

Substituting for $[G]$ in terms of Hermite polynomials the stiffness matrix $[k]$ becomes

$$[k] = \int_0^a \int_0^b e^{i2\lambda^*(ct-x)} \begin{bmatrix}
H^{(1)}_{o1}(y)\,(H^{(1)\prime}_{o1}(x) - i\lambda^* H^{(1)}_{o1}(x)) & H^{(1)}_{o1}(x)\,H^{(1)\prime}_{o1}(y) \\
H^{(1)}_{o1}(y)\,(H^{(1)\prime}_{i1}(x) - i\lambda^* H^{(1)}_{i1}(x)) & H^{(1)}_{i1}(x)\,H^{(1)\prime}_{o1}(y) \\
H^{(1)}_{i1}(y)\,(H^{(1)\prime}_{i1}(x) - i\lambda^* H^{(1)}_{o1}(x)) & H^{(1)}_{o1}(x)\,H^{(1)\prime}_{i1}(y) \\
H^{(1)}_{o1}(y)\,(H^{(1)\prime}_{o2}(x) - i\lambda^* H^{(1)}_{o2}(x)) & H^{(1)}_{o2}(x)\,H^{(1)\prime}_{o1}(y) \\
H^{(1)}_{o1}(y)\,(H^{(1)\prime}_{i2}(x) - i\lambda^* H^{(1)}_{i2}(x)) & H^{(1)}_{i2}(x)\,H^{(1)\prime}_{o1}(y) \\
H^{(1)}_{i1}(y)\,(H^{(1)\prime}_{i2}(x) - i\lambda^* H^{(1)}_{o2}(x)) & H^{(1)}_{o2}(x)\,H^{(1)\prime}_{i1}(y) \\
H^{(1)}_{o2}(y)\,(H^{(1)\prime}_{o1}(x) - i\lambda^* H^{(1)}_{o1}(x)) & H^{(1)}_{o1}(x)\,H^{(1)\prime}_{o2}(y) \\
H^{(1)}_{o2}(y)\,(H^{(1)\prime}_{i1}(x) - i\lambda^* H^{(1)}_{i1}(x)) & H^{(1)}_{i1}(x)\,H^{(1)\prime}_{o2}(y) \\
H^{(1)}_{i2}(y)\,(H^{(1)\prime}_{o1}(x) - i\lambda^* H^{(1)}_{o1}(x)) & H^{(1)}_{o1}(x)\,H^{(1)\prime}_{i2}(y) \\
H^{(1)}_{o2}(y)\,(H^{(1)\prime}_{o2}(x) - i\lambda^* H^{(1)}_{o2}(x)) & H^{(1)}_{o2}(x)\,H^{(1)\prime}_{o2}(y) \\
H^{(1)}_{o2}(y)\,(H^{(1)\prime}_{i2}(x) - i\lambda^* H^{(1)}_{i2}(x)) & H^{(1)}_{i2}(x)\,H^{(1)\prime}_{i2}(y) \\
H^{(1)}_{i2}(y)\,(H^{(1)\prime}_{o2}(x) - i\lambda^* H^{(1)}_{o2}(x)) & H^{(1)}_{o2}(x)\,H^{(1)\prime}_{i2}(y)
\end{bmatrix}$$

$$\begin{bmatrix} \frac{\partial^2}{\partial x^2} & 0 \\ 0 & \frac{\partial^2}{\partial y^2} \end{bmatrix} \cdot \begin{bmatrix} H^{(1)}_{o1}(y)\left(H^{(1)\prime}_{o1}(x) - i\lambda^* H^{(1)}_{o1}(x)\right) & H^{(1)}_{o1}(y)\left(H^{(1)\prime}_{o2}(x) - i\lambda^* H^{(1)}_{o2}(x)\right) \\ H^{(1)}_{o1}(x) H^{(1)\prime}_{o1}(y) & H^{(1)}_{o2}(x) H^{(1)\prime}_{o1}(y) \end{bmatrix}$$

$$\begin{bmatrix} H^{(1)}_{o1}(y)\left(H^{(1)\prime}_{o1}(x) - i\lambda^* H^{(1)}_{o1}(x)\right) & H^{(1)}_{o1}(y)\left(H^{(1)\prime}_{o2}(x) - i\lambda^* H^{(1)}_{o2}(x)\right) \\ H^{(1)}_{o1}(x) H^{(1)\prime}_{o1}(y) & H^{(1)}_{o2}(x) H^{(1)\prime}_{o1}(y) \end{bmatrix}$$

$$\begin{bmatrix} H^{(1)}_{o1}(y)\left(H^{(1)\prime}_{i2}(x) - i\lambda^* H^{(1)}_{i2}(x)\right) & H^{(1)}_{i1}(y)\left(H^{(1)\prime}_{o2}(x) - i\lambda^* H^{(1)}_{o2}(x)\right) \\ H^{(1)}_{i2}(x) H^{(1)\prime}_{i1}(y) & H^{(1)}_{o2}(x) H^{(1)\prime}_{i1}(y) \end{bmatrix}$$

$$\begin{bmatrix} H^{(1)}_{i2}(x)\left(H^{(1)\prime}_{i1}(x) - i\lambda^* H^{(1)}_{o1}(x)\right) & H^{(1)}_{o2}(x)\left(H^{(1)\prime}_{i1}(x) - i\lambda^* H^{(1)}_{i1}(x)\right) \\ H^{(1)}_{i1}(x) H^{(1)\prime}_{i2}(y) & H^{(1)}_{i1}(x) H^{(1)\prime}_{o2}(y) \end{bmatrix}$$

$$\begin{bmatrix} H^{(1)}_{i1}(y)\left(H^{(1)\prime}_{o2}(x) - i\lambda^* H^{(1)}_{o2}(x)\right) & H^{(1)}_{i2}(y)\left(H^{(1)\prime}_{o2}(x) - i\lambda^* H^{(1)}_{o2}(x)\right) \\ H^{(1)}_{o2}(x) H^{(1)\prime}_{o2}(y) & H^{(1)}_{o2}(x) H^{(1)\prime}_{o2}(y) \end{bmatrix}$$

$$\begin{bmatrix} H^{(1)}_{o2}(y)\left(H^{(1)\prime}_{i2}(x) - i\lambda^* H^{(1)}_{i2}(x)\right) & H^{(1)}_{i2}(y)\left(H^{(1)\prime}_{o2}(x) - i\lambda^* H^{(1)}_{o2}(x)\right) \\ H^{(1)}_{i2}(x) H^{(1)\prime}_{o2}(y) & H^{(1)}_{i2}(x) H^{(1)\prime}_{i2}(y) \end{bmatrix} dx\,dy$$

(A-1)

Substituting for the $H^{N}_{ki}(x)$ from Eqn.(3.1) in terms of [illegible] and by integrating Eqn. (A-1) term by term the whole [k] matrix is known. The detailed calculations involved in integration are illustrated here for one element.

$$k_{11} = \int_0^a \int_0^b e^{i2\lambda^*(ct-x)} \left(T_x^0 H_{01}^{(1)2}(y) \left(H_{01}^{(1)}(x) - i\lambda^* H_{01}^{(1)}(x) \right)^2 + T_y^0 H_{01}^{(1)2}(x) H_{01}^{(1)2}(y) \right) dx\,dy$$

$$= \int_0^a \int_0^b e^{i2\lambda^*(ct-x)} \left[\frac{T_x^0}{a^6 b^6} \left((2y^3 - 3by^2 + b^3)^2 \left\{ (6x^2 - 6ax) - i\lambda^* (2x^3 - 3ax^2 + a^3) \right\}^2 \right) \right.$$

$$\left. + \frac{T_y^0}{a^6 b^6} (2x^3 - 3ax^2 + a^3)^2 (6y^2 - 6by)^2 \right] dx\,dy$$

$$= e^{2i\lambda^* ct} \left\{ \int_0^b \left[\frac{T_x^0}{a^6 b^6} \int_0^a e^{-i2\lambda^* x} \left(-4\lambda^{*2} x^6 - 12(-a\lambda^{*2} + i2\lambda^*) x^5 + \right. \right. \right.$$

$$3(12 - 3a^2\lambda^{*2} + 20a\lambda^*) x^4 - 4(18a + a^3\lambda^{*2} + i9a^2\lambda^*) x^3 +$$

$$\left. \left. \left. (a^2(4 + a^2\lambda^{*2} - i2a\lambda^*) x^2 + i12a^4\lambda^* x - a^6\lambda^{*2}) dx \right] (2y^3 - 3by^2 + b^3)^2 dy \right.$$

$$+ \int_0^b \left[\frac{T_y^0}{a^6 b^6} \int_0^a e^{-i2\lambda^* x} \left(11x^6 - 12ax^5 + 9a^2 x^4 + 4a^3 x^3 - 6a^4 x^2 + a^6 \right) dx \right] \cdot$$

$$\left. 36(y^2 - by)^2 dy \right\}$$

on integration and substitution of limits, k_{11} becomes

$$k_{11} = e^{i2\lambda^* ct} \left[T_x^0 F_1(\lambda^*) + T_y^0 F_2(\lambda^*) \right]$$

Similarly the other elements can be calculated by carrying out such integrations. For them direct results will be given here. Since [k] is a symmetric matrix so only the elements of lower triangle will be given. They are as follows:

$$k_{21} = e^{i2\lambda^* ct}\left[T_x^\circ F_3(\lambda^*) + T_y^\circ F_4(\lambda^*)\right]; \quad k_{22} = e^{i2\lambda^* ct}\left[T_x^\circ F_5(\lambda^*) + T_y^\circ F_6(\lambda^*)\right]$$

$$k_{31} = e^{i2\lambda^* ct}\left[T_x^\circ\left(\frac{11b}{78}F_1(\lambda^*)\right) + T_y^\circ\left(\frac{b}{12}F_2(\lambda^*)\right)\right]; \quad k_{32} = e^{i2\lambda^* ct}\left[T_x^\circ\left(\frac{11b}{78}F_3(\lambda^*)\right) + T_y^\circ\left(\frac{b}{12}F_4(\lambda^*)\right)\right]$$

$$k_{33} = e^{i2\lambda^* ct}\left[T_x^\circ\left(\frac{b^2}{39}F_1(\lambda^*)\right) + T_y^\circ\left(\frac{b^2}{9}F_2(\lambda^*)\right)\right]; \quad k_{41} = e^{i2\lambda^* ct}\left[T_x^\circ F_7(\lambda^*) + T_y^\circ F_8(\lambda^*)\right]$$

$$k_{42} = e^{i2\lambda^* ct}\left[T_x^\circ F_9(\lambda^*) + T_y^\circ F_{10}(\lambda^*)\right]; \quad k_{43} = e^{i2\lambda^* ct}\left[T_x^\circ\left(\frac{11b}{78}F_7(\lambda^*)\right) + T_y^\circ\left(\frac{b}{12}F_8(\lambda^*)\right)\right]$$

$$k_{44} = e^{i2\lambda^* ct}\left[T_x^\circ F_{11}(\lambda^*) + T_y^\circ F_{12}(\lambda^*)\right]; \quad k_{51} = e^{i2\lambda^* ct}\left[T_x^\circ F_{13}(\lambda^*) + T_y^\circ F_{14}(\lambda^*)\right]$$

$$k_{52} = e^{i2\lambda^* ct}\left[T_x^\circ F_{15}(\lambda^*) + T_y^\circ F_{16}(\lambda^*)\right]; \quad k_{53} = e^{i2\lambda^* ct}\left[T_x^\circ\left(\frac{11b}{78}F_{13}(\lambda^*)\right) + T_y^\circ\left(\frac{b}{12}F_{14}(\lambda^*)\right)\right]$$

$$k_{54} = e^{i2\lambda^* ct}\left[T_x^\circ F_{17}(\lambda^*) + T_y^\circ F_{18}(\lambda^*)\right]; \quad k_{55} = e^{i2\lambda^* ct}\left[T_x^\circ F_{19}(\lambda^*) + T_y^\circ F_{20}(\lambda^*)\right]$$

$$k_{61} = e^{i2\lambda^* ct}\left[T_x^\circ\left(\frac{11b}{78}F_7(\lambda^*)\right) + T_y^\circ\left(\frac{b}{12}F_8(\lambda^*)\right)\right]$$

$$k_{62} = e^{i2\lambda^* ct}\left[T_x^\circ\left(\frac{11b}{78}F_9(\lambda^*)\right) + T_y^\circ\left(\frac{b}{12}F_{10}(\lambda^*)\right)\right]$$

$$k_{63} = e^{i2\lambda^* ct}\left[T_x^\circ\left(\frac{b^2}{39}F_7(\lambda^*)\right) + T_y^\circ\left(\frac{b^2}{9}F_8(\lambda^*)\right)\right]$$

$$k_{64} = e^{i2\lambda^* ct}\left[T_x^\circ\left(\frac{11b}{78}F_{11}(\lambda^*)\right) + T_y^\circ\left(\frac{b}{12}F_{12}(\lambda^*)\right)\right]$$

$$k_{15} = e^{i\theta\lambda^* ct}\left[T_x^\circ\left(\frac{11b}{78}F_{17}(\lambda^*)\right) + T_y^\circ\left(\frac{b}{12}F_{18}(\lambda^*)\right)\right]$$

$$k_{16} = e^{i\theta\lambda^* ct}\left[T_x^\circ\left(\frac{b^2}{39}F_{11}(\lambda^*)\right) + T_y^\circ\left(\frac{b^2}{9}F_{12}(\lambda^*)\right)\right]$$

$$k_{71} = e^{i\theta\lambda^* ct}\left[T_x^\circ\left(\frac{9}{2\ell}F_1(\lambda^*) - T_y^\circ F_2(\lambda^*)\right]\right.$$

$$k_{72} = e^{i2\lambda^* ct}\left[T_x^\circ\left(\frac{9}{2\ell}F_3(\lambda^*)\right) - T_y^\circ F_4(\lambda^*)\right]$$

$$k_{73} = e^{i2\lambda^* ct}\left[T_x^\circ\left(\frac{b}{12}F_1(\lambda^*) - T_y^\circ\left(\frac{b}{12}F_2(\lambda^*)\right)\right]\right.$$

$$k_{74} = e^{i2\lambda^* ct}\left[T_x^\circ\left(\frac{9}{2\ell}F_7(\lambda^*)\right) - T_y^\circ F_8(\lambda^*)\right]$$

$$k_{75} = e^{i2\lambda^* ct}\left[T_x^\circ\left(\frac{9}{2\ell}F_{13}(\lambda^*)\right) - T_y^\circ F_{14}(\lambda^*)\right]$$

$$k_{76} = e^{i2\lambda^* ct}\left[T_x^\circ\left(\frac{b}{12}F_7(\lambda^*)\right) - T_y^\circ\left(\frac{b}{12}F_8(\lambda^*)\right)\right]$$

$$k_{77} = k_{11} \quad ; \quad k_{81} = k_{72} \; ; \; k_{82} = e^{i2\lambda^* ct}\left[T_x^\circ\left(\frac{9}{2\ell}F_5(\lambda^*)\right) - T_y^\circ F_6(\lambda^*)\right]$$

$$k_{83} = e^{i2\lambda^* ct}\left[T_x^\circ\left(\frac{b}{12}F_3(\lambda^*)\right) - T_y^\circ\left(\frac{b}{12}F_4(\lambda^*)\right)\right]$$

$$k_{84} = e^{i2\lambda^* ct}\left[T_x^\circ\left(\frac{9}{2\ell}F_9(\lambda^*)\right) - T_y^\circ F_{10}(\lambda^*)\right]$$

$$k_{85} = e^{i2\lambda^* ct}\left[T_x^\circ\left(\frac{9}{2\ell}F_{15}(\lambda^*)\right) - T_y^\circ F_{16}(\lambda^*)\right]$$

$$k_{86} = e^{i2\lambda^* ct}\left[T_x^\circ\left(\frac{b}{12}F_9(\lambda^*)\right) - T_y^\circ\left(\frac{b}{12}F_{10}(\lambda^*)\right)\right]$$

$k_{87} = k_{21}$; $k_{88} = k_{22}$; $k_{81} = -k_{73}$

$k_{82} = e^{i2\lambda^* ct}\left[-T_x^\circ\left(\frac{b}{12}F_3(\lambda^*)\right) + T_y^\circ\left(\frac{b}{12}F_4(\lambda^*)\right)\right] = -k_{83}$

$k_{83} = e^{i2\lambda^* ct}\left[T_x^\circ\left(\frac{b^2}{52}F_1(\lambda^*)\right) + T_y^\circ\left(\frac{b^2}{36}F_2(\lambda^*)\right)\right]$

$k_{84} = -k_{76}$; $k_{85} = e^{i2\lambda^* ct}\left[-T_x^\circ\left(\frac{b}{12}F_{13}(\lambda^*)\right) + T_y^\circ\left(\frac{b}{12}F_{14}(\lambda^*)\right)\right]$

$k_{86} = -e^{i2\lambda^* ct}\left[T_x^\circ\left(\frac{b^2}{52}F_7(\lambda^*)\right) + T_y^\circ\left(\frac{b^2}{36}F_8(\lambda^*)\right)\right]$

$k_{87} = -k_{31}$; $k_{88} = -k_{32}$; $k_{89} = k_{33}$

$k_{10,1} = k_{74}$; $k_{10,2} = k_{84}$; $k_{10,3} = k_{76}$

$k_{10,4} = e^{i2\lambda^* ct}\left[T_x^\circ\left(\frac{9}{26}F_{11}(\lambda^*)\right) - T_y^\circ F_{12}(\lambda^*)\right]$

$k_{10,5} = e^{i2\lambda^* ct}\left[T_x^\circ\left(\frac{9}{26}F_{17}(\lambda^*)\right) - T_y^\circ F_{18}(\lambda^*)\right]$

$k_{10,6} = e^{i2\lambda^* ct}\left[T_x^\circ\left(\frac{b}{12}F_{11}(\lambda^*)\right) - T_y^\circ\left(\frac{b}{12}F_{12}(\lambda^*)\right)\right]$

$k_{10,7} = k_{41}$; $k_{10,8} = k_{42}$; $k_{10,9} = -k_{43}$; $k_{10,10} = k_{44}$

$k_{11,1} = k_{75}$; $k_{11,2} = k_{85}$; $k_{11,3} = -k_{95}$; $k_{11,4} = k_{10,5}$

$k_{11,5} = e^{i2\lambda^* ct}\left[T_x^\circ\left(\frac{9}{26}F_{19}(\lambda^*)\right) - T_y^\circ F_{20}(\lambda^*)\right]$

$k_{11,6} = e^{i2\lambda^* ct}\left[T_x^\circ\left(\frac{b}{12}F_{19}(\lambda^*)\right) - T_y^\circ\left(\frac{b}{12}F_{18}(\lambda^*)\right)\right]$

$k_{11,7} = k_{51}$; $k_{11,8} = k_{52}$; $k_{11,9} = -k_{53}$; $k_{11,10} = k_{54}$; $k_{11,11} = k_{55}$

$k_{12,1} = -k_{76}$; $k_{12,2} = -k_{86}$; $k_{12,3} = k_{96}$; $k_{12,4} = -k_{10,6}$

$k_{12,5} = -k_{11,6}$; $k_{12,6} = -e^{i2\lambda^* ct}\left[T_x^\circ\left(\frac{b^2}{52} F_{116}(\lambda^*)\right) + T_y^\circ\left(\frac{b^2}{36} F_{126}(\lambda^*)\right)\right]$

$k_{12,7} = k_{10,9}$; $k_{12,8} = -k_{62}$; $k_{12,9} = k_{63}$; $k_{12,10} = -k_{64}$;

$k_{12,11} = -k_{65}$; $k_{12,12} = k_{66}$.

Where

$$F_1(\lambda^*) = \left(\frac{1}{a^6 b^6}\right)\left(\frac{13}{35} b^7\right)\left[\left(\frac{-i2\lambda^* a}{\frac{ie}{2\lambda^*}}\right)\left(-\frac{9}{2}\frac{a^2}{\lambda^{*2}} + i9\frac{a}{\lambda^{*3}} + 9\frac{1}{\lambda^{*4}}\right) + \left(i\frac{1}{2}a^6\lambda^* - i\frac{3}{2}\frac{a^4}{\lambda^*} + \frac{3}{2}\frac{a^3}{\lambda^{*2}} + i\frac{9}{4}\frac{a^2}{\lambda^{*3}} - \frac{9}{2}\frac{a}{\lambda^{*4}} - i\frac{9}{2}\frac{1}{\lambda^{*5}}\right)\right]$$

$$F_2(\lambda^*) = \frac{1}{a^6 b^6}\left(\frac{6}{5} b^5\right)\left[\left(\frac{-i2\lambda^* a}{\frac{ie}{2\lambda^*}}\right)\left(\frac{27}{2}\frac{a^2}{\lambda^{*4}} - i45\frac{a}{\lambda^{*5}} - 45\frac{1}{\lambda^{*6}}\right) + \left(-i\frac{1}{2}\frac{a^6}{\lambda^*} - i\frac{3}{2}\frac{a^4}{\lambda^{*3}} + \frac{3}{2}\frac{a^3}{\lambda^{*4}} - i\frac{27}{4}\frac{a^2}{\lambda^{*5}} + \frac{45}{2}\frac{a}{\lambda^{*6}} + \frac{45}{2}\frac{1}{\lambda^{*7}}\right)\right]$$

$$F_3(\lambda^*) = \left(\frac{1}{a^5 b^6}\right)\left(\frac{13}{35} b^7\right)\left[\left(\frac{-i2\lambda^* a}{\frac{ie}{2\lambda^*}}\right)\left(-a^6\lambda^{*2} - i\frac{3}{2}a^5\lambda^* + \frac{3}{2}a^4 - i\frac{3}{4}\frac{a^3}{\lambda^*} - \frac{3}{2}\frac{a^2}{\lambda^{*2}} + i\frac{15}{4}\frac{a}{\lambda^{*3}} + \frac{9}{2}\frac{1}{\lambda^{*4}}\right) + \left(-\frac{1}{4}a^5 - i\frac{1}{2}\frac{a^4}{\lambda^*} + \frac{3}{8}\frac{a^3}{\lambda^{*2}} + i\frac{3}{2}\frac{a^2}{\lambda^{*3}} - \frac{91}{8}\frac{a}{\lambda^{*4}} - i\frac{9}{4}\frac{1}{\lambda^{*5}}\right)\right]$$

$$F_4(\lambda^*) = \left(\frac{1}{a^5 b^6}\right)\left(\frac{6}{5}b^5\right)\left[\left(\frac{ie^{-i2\lambda^* a}}{2\lambda^*}\right)\left(\frac{9}{2}\frac{a^2}{\lambda^{*4}} - i\frac{75}{4}\frac{a}{\lambda^{*5}} - \frac{45}{2}\frac{1}{\lambda^{*6}}\right)\right.$$
$$\left. + \left(-\frac{1}{4}\frac{a^5}{\lambda^{*2}} - i\frac{1}{2}\frac{a^4}{\lambda^{*3}} - \frac{3}{4}\frac{a^3}{\lambda^{*4}} - i\frac{6}{5}\frac{a^2}{\lambda^{*5}} + \frac{105}{8}\frac{a}{\lambda^{*6}} + i\frac{45}{4}\frac{1}{\lambda^{*7}}\right)\right]$$

$$F_5(\lambda^*) = \left(\frac{1}{a^4 b^6}\right)\left(\frac{13}{35}b^7\right)\left[\left(\frac{ie^{-i2\lambda^* a}}{2\lambda^*}\right)\left(-\frac{1}{2}\frac{a^2}{\lambda^{*2}} + i\frac{3}{2}\frac{a}{\lambda^{*3}} + \frac{9}{4}\frac{1}{\lambda^{*4}}\right) + \left(-i\frac{1}{4}\frac{a^4}{\lambda^{*}}\right.\right.$$
$$\left.\left. + \frac{1}{2}\frac{a^3}{\lambda^{*2}} + i\frac{a^2}{\lambda^{*3}} - \frac{3}{2}\frac{a}{\lambda^{*4}} - i\frac{9}{8}\frac{1}{\lambda^{*5}}\right)\right]$$

$$F_6(\lambda^*) = \left(\frac{1}{a^4 b^6}\right)\left(\frac{6}{5}b^5\right)\left[\left(\frac{ie^{-i2\lambda^* a}}{2\lambda^*}\right)\left(\frac{3}{2}\frac{a^2}{\lambda^{*4}} - i\frac{15}{2}\frac{a}{\lambda^{*5}} - \frac{45}{4}\frac{1}{\lambda^{*6}}\right) +\right.$$
$$\left.\left(i\frac{1}{4}\frac{a^4}{\lambda^{*3}} - \frac{3}{2}\frac{a^3}{\lambda^{*4}} - i\frac{9}{2}\frac{a^2}{\lambda^{*5}} + \frac{15}{2}\frac{a}{\lambda^{*6}} + i\frac{45}{8}\frac{1}{\lambda^{*7}}\right)\right]$$

$$F_7(\lambda^*) = \left(\frac{1}{a^{16} b^6}\right)\left(\frac{13}{35}b^7\right)\left[\left(\frac{ie^{-i2\lambda^* a}}{2\lambda^*}\right)\left(-\frac{3}{2}a^4 + i\frac{3}{2}\frac{a^3}{\lambda^*} + \frac{9}{2}\frac{a^2}{\lambda^{*2}} - i9\frac{a}{\lambda^{*3}} - 9\frac{1}{\lambda^{*4}}\right)\right.$$
$$\left. + \left(\frac{13}{8}\frac{a^4}{\lambda^*} - \frac{3}{4}\frac{a^3}{\lambda^{*2}} - i\frac{9}{4}\frac{a^2}{\lambda^{*3}} + \frac{9}{2}\frac{a}{\lambda^{*4}} + i\frac{9}{2}\frac{1}{\lambda^{*5}}\right)\right]$$

$$F_8(\lambda^*) = \left(\frac{1}{a^{16} b^6}\right)\left(\frac{6}{5}b^5\right)\left[\left(\frac{ie^{-i2\lambda^* a}}{2\lambda^*}\right)\left(\frac{3}{2}\frac{a^4}{\lambda^{*2}} - i\frac{3}{2}\frac{a^3}{\lambda^{*3}} + \frac{27}{2}\frac{a^2}{\lambda^{*4}} - i45\frac{a}{\lambda^{*5}}\right.\right.$$
$$\left.\left. - 105\frac{1}{\lambda^{*6}}\right) + \left(-i\frac{3}{4}\frac{a^4}{\lambda^{*3}} + \frac{3}{4}\frac{a^3}{\lambda^{*4}} - i\frac{27}{4}\frac{a^2}{\lambda^{*5}} + \frac{45}{2}\frac{a}{\lambda^{*6}} + i\frac{45}{2}\frac{1}{\lambda^{*7}}\right)\right]$$

$$F_9(\lambda^*) = \left(\frac{1}{a^5 b^6}\right)\left(\frac{13}{35}b^7\right)\left[\left(\frac{ie^{-i2\lambda^* a}}{2\lambda^*}\right)\left(-\frac{a^4}{2} + i\frac{3}{4}\frac{a^3}{\lambda^*} + \frac{3}{2}\frac{a^2}{\lambda^{*2}} - i\frac{15}{4}\frac{a}{\lambda^{*3}} - \frac{9}{2}\frac{1}{\lambda^{*4}}\right)\right.$$
$$\left. + \left(-\frac{3}{8}\frac{a^3}{\lambda^{*2}} - i\frac{3}{2}\frac{a^2}{\lambda^{*3}} + \frac{21}{8}\frac{a}{\lambda^{*4}} + i\frac{9}{4}\frac{1}{\lambda^{*5}}\right)\right]$$

$$F_{10}(\lambda^*) = \left(\frac{1}{a^5 b^6}\right)\left(\frac{6}{5}b^5\right)\left[\left(\frac{ie^{-i2\lambda^* a}}{2\lambda^*}\right)\left(\frac{1}{2}\frac{a^4}{\lambda^{*2}} - i\frac{3}{4}\frac{a^3}{\lambda^{*3}} + \frac{9}{2}\frac{a^2}{\lambda^{*4}} - i\frac{9}{4}\frac{a}{\lambda^{*5}} -\right.\right.$$
$$\left.\left. 15\frac{1}{\lambda^{*6}}\right) + \left(-\frac{9}{8}\frac{a^3}{\lambda^{*4}} - i6\frac{a^2}{\lambda^{*5}} + \frac{105}{8}\frac{a}{\lambda^{*6}} + i\frac{45}{4}\frac{1}{\lambda^{*7}}\right)\right]$$

$$F_{11}(\lambda^*) = \left(\frac{1}{a^6 b^6}\right)\left(\frac{13}{35}b^7\right)\left[\left(\frac{ie^{-i2\lambda^* a}}{2\lambda^*}\right)\left(-a^6\lambda^{*2} + 3a^4 - i3\frac{a^3}{\lambda^*} - \frac{9}{2}\frac{a^2}{\lambda^{*2}} + i9\frac{a}{\lambda^{*3}} + \frac{9}{\lambda^{*4}}\right) + \left(i\frac{9}{4}\frac{a^2}{\lambda^{*3}} - \frac{9}{2}\frac{a}{\lambda^{*4}} - i\frac{9}{2}\frac{1}{\lambda^{*5}}\right)\right]$$

$$F_{12}(\lambda^*) = \left(\frac{1}{a^6 b^6}\right)\left(\frac{6}{5}b^5\right)\left[\left(\frac{ie^{-i2\lambda^* a}}{2\lambda^*}\right)\left(a^6 + 3\frac{a^4}{\lambda^{*2}} - i3\frac{a^3}{\lambda^{*3}} - \frac{27}{2}\frac{a^2}{\lambda^{*4}} - i45\frac{a}{\lambda^{*5}} - 45\frac{1}{\lambda^{*6}}\right) + \left(-i\frac{27}{4}\frac{a^2}{\lambda^{*5}} + \frac{45}{2}\frac{a}{\lambda^{*6}} + i\frac{45}{2}\frac{1}{\lambda^{*7}}\right)\right]$$

$$F_{13}(\lambda^*) = \left(\frac{1}{a^5 b^6}\right)\left(\frac{13}{35}b^7\right)\left[\left(\frac{ie^{-i2\lambda^* a}}{2\lambda^*}\right)\left(-i\frac{3}{4}\frac{a^3}{\lambda^*} - 3\frac{a^2}{\lambda^{*2}} + i\frac{21}{4}\frac{a}{\lambda^{*3}} + \frac{9}{2}\frac{1}{\lambda^{*4}}\right) + \left(-i\frac{1}{4}\frac{a^4}{\lambda^*} + \frac{3}{8}\frac{a^3}{\lambda^{*2}} - i\frac{3}{4}\frac{a^2}{\lambda^{*3}} - \frac{15}{8}\frac{a}{\lambda^{*4}} - i\frac{9}{4}\frac{1}{\lambda^{*5}}\right)\right]$$

$$F_{14}(\lambda^*) = \left(\frac{1}{a^5 b^6}\right)\left(\frac{6}{5}b^5\right)\left[\left(\frac{ie^{-i2\lambda^* a}}{2\lambda^*}\right)\left(i\frac{9}{4}\frac{a^3}{\lambda^{*3}} + 12\frac{a^2}{\lambda^{*4}} - i\frac{105}{4}\frac{a}{\lambda^{*5}} - \frac{45}{2}\frac{1}{\lambda^{*6}}\right) + \left(-i\frac{1}{4}\frac{a^4}{\lambda^{*3}} + \frac{3}{8}\frac{a^3}{\lambda^{*4}} - i\frac{9}{4}\frac{a^2}{\lambda^{*5}} + \frac{75}{8}\frac{a}{\lambda^{*6}} + i\frac{45}{4}\frac{1}{\lambda^{*7}}\right)\right]$$

$$F_{15}(\lambda^*) = \left(\frac{1}{a^4 b^6}\right)\left(\frac{13}{35}b^7\right)\left[\left(\frac{ie^{-i2\lambda^* a}}{2\lambda^*}\right)\left(-i\frac{1}{4}\frac{a^3}{\lambda^*} - \frac{a^2}{\lambda^{*2}} - i\frac{9}{4}\frac{a}{\lambda^{*3}} + \frac{9}{4}\frac{1}{\lambda^{*4}}\right) + \left(\frac{1}{8}\frac{a^3}{\lambda^{*2}} + i\frac{1}{2}\frac{a^2}{\lambda^{*3}} - \frac{9}{8}\frac{a}{\lambda^{*4}} - i\frac{9}{8}\frac{1}{\lambda^{*5}}\right)\right]$$

$$F_{16}(\lambda^*) = \left(\frac{1}{a^4 b^6}\right)\left(\frac{6}{5}b^5\right)\left[\left(\frac{ie^{-i2\lambda^* a}}{2\lambda^*}\right)\left(i\frac{3}{4}\frac{a^3}{\lambda^{*3}} + \frac{9}{2}\frac{a^2}{\lambda^{*4}} - i\frac{45}{4}\frac{a}{\lambda^{*5}} - \frac{45}{4}\frac{1}{\lambda^{*6}}\right) + \left(-\frac{3}{8}\frac{a^3}{\lambda^{*4}} - i\frac{9}{4}\frac{a^2}{\lambda^{*5}} + \frac{45}{8}\frac{a}{\lambda^{*6}} + i\frac{45}{8}\frac{1}{\lambda^{*7}}\right)\right]$$

$$F_{17}(\lambda^*) = \left(\frac{1}{a^5 b^6}\right)\left(\frac{13}{35}b^7\right)\left[\left(\frac{ie^{-i2\lambda^* a}}{2\lambda^*}\right)\left(-i\frac{1}{2}a^5\lambda^* - a^4 - i\frac{11}{2}\frac{a^3}{\lambda^*} - 3\frac{a^2}{\lambda^{*2}} - i\frac{91}{4}\frac{a}{\lambda^{*3}} - \frac{9}{2}\frac{1}{\lambda^{*4}}\right) + \left(-i\frac{3}{4}\frac{a^2}{\lambda^{*3}} + \frac{15}{8}\frac{a}{\lambda^{*4}} - \frac{9}{4}\right)\right]$$

$$F_{18}(\lambda^*) = \left(\frac{1}{a^5 b^6}\right)\left(\frac{1}{5}b^6\right)\left[\left(\frac{ie^{-i2\lambda^* a}}{2\lambda^*}\right)\left(i\frac{1}{2}a^5\lambda^* - \frac{a^4}{\lambda^{*2}} - i\frac{3}{2}\frac{a^3}{\lambda^{*3}} - 12\frac{a^2}{\lambda^{*4}} + i\frac{105}{4}\frac{a}{\lambda^{*5}} + \frac{45}{2}\frac{1}{\lambda^{*6}}\right) + \left(i\frac{9}{4}\frac{a^2}{\lambda^{*5}} - \frac{75}{8}\frac{a}{\lambda^{*6}} - i\frac{45}{4}\frac{1}{\lambda^{*7}}\right)\right]$$

$$F_{19}(\lambda^*) = \left(\frac{1}{a^6 b^6}\right)\left(\frac{13}{35}b^7\right)\left[\left(\frac{ie^{-i2\lambda^* a}}{2\lambda^*}\right)\left(\frac{a^4}{2} - i\frac{a^3}{\lambda^*} - 2\frac{a^2}{\lambda^{*2}} + i3\frac{a}{\lambda^{*3}} + \frac{9}{4}\frac{1}{\lambda^{*4}}\right) + \left(i\frac{1}{4}\frac{a^2}{\lambda^{*3}} - \frac{3}{4}\frac{a}{\lambda^{*4}} - i\frac{9}{8}\frac{1}{\lambda^{*5}}\right)\right]$$

$$F_{20}(\lambda^*) = \left(\frac{1}{a^4 b^6}\right)\left(\frac{1}{5}b^5\right)\left[\left(\frac{ie^{-i2\lambda^* a}}{2\lambda^*}\right)\left(-\frac{1}{2}\frac{a^4}{\lambda^{*2}} + i3\frac{a^3}{\lambda^{*3}} + 9\frac{a^2}{\lambda^{*4}} - i15\frac{a}{\lambda^{*5}} - \frac{45}{4}\frac{1}{\lambda^{*6}}\right) + \left(-i\frac{3}{4}\frac{a^2}{\lambda^{*5}} + \frac{15}{4}\frac{a}{\lambda^{*6}} + i\frac{45}{8}\frac{1}{\lambda^{*7}}\right)\right]$$

Mass Matrix:

Rewriting the equation (4.29) for mass matrix, we get

$$[m] = \rho_m h \int_0^a \int_0^b e^{-i2\lambda^* x} \{f\}\{f\}^T \, dx \, dy$$

where $\{f\}$ is given by Eqn. (3.7). $[m]$ is written in terms of Hermite polynomials as in Eqn. (A.2)

$$[m]^{(1)} = \rho_m h \, e^{i\ell\lambda^* ct} \int_0^a \int_0^b e^{-i\ell\lambda^* x} \left\{ \begin{array}{l} H_{o1}^{(1)}(x)\, H_{o1}^{(1)}(y) \\ H_{11}^{(1)}(x)\, H_{o1}(y) \\ H_{o1}^{(1)}(x)\, H_{11}^{(1)}(y) \\ H_{o2}^{(1)}(x)\, H_{o1}^{(1)}(y) \\ H_{12}^{(1)}(x)\, H_{o1}^{(1)}(y) \\ H_{o2}^{(1)}(x)\, H_{11}^{(1)}(y) \\ H_{o1}^{(1)}(x)\, H_{o2}^{(1)}(y) \\ H_{11}^{(1)}(x)\, H_{o2}^{(1)}(y) \\ H_{o1}^{(1)}(x)\, H_{12}^{(1)}(y) \\ H_{o2}^{(1)}(x)\, H_{o2}^{(1)}(y) \\ H_{12}^{(1)}(x)\, H_{o2}^{(1)}(y) \\ H_{o2}^{(1)}(x)\, H_{12}^{(1)}(y) \end{array} \right\} \cdot \left[\begin{array}{llll} H_{11}^{(1)}(x)\, H_{o1}^{(1)}(y) & H_{o1}^{(1)}(x)\, H_{11}^{(1)}(y) & H_{o2}^{(1)}(x)\, H_{o1}^{(1)}(y) & H_{12}^{(1)}(x)\, H_{o1}^{(1)}(y) \\ H_{o2}^{(1)}(x)\, H_{11}^{(1)}(y) & H_{o1}^{(1)}(x)\, H_{o2}^{(1)}(y) & H_{11}^{(1)}(x)\, H_{o2}^{(1)}(y) & H_{o1}^{(1)}(x)\, H_{12}^{(1)}(y) \\ H_{o2}^{(1)}(x)\, H_{o2}^{(1)}(y) & H_{12}^{(1)}(x)\, H_{o2}^{(1)}(y) & H_{o2}^{(1)}(x)\, H_{12}^{(1)}(y) & \end{array} \right] dx\, dy$$

(A·2)

Substituting for these polynomials from Eqn. (3.1) and then integrating term by term, we can get all the elements of the mass matrix, on substituting the limits. This is also a symmetric matrix. So the elements corresponding to its lower triangle are given as follows:

$m_{11} = f_m h e^{i2\lambda^* ct} \cdot \frac{13}{42} b^2 F_2(\lambda^*)$; $m_{21} = f_m h e^{i2\lambda^* ct} \cdot \frac{13}{42} b^2 F_4(\lambda^*)$

$m_{22} = f_m h e^{i2\lambda^* ct} \cdot \frac{13}{42} b^2 F_6(\lambda^*)$; $m_{31} = f_m h e^{i2\lambda^* ct} \cdot \frac{11}{6\times 42} b^3 F_2(\lambda^*)$

$m_{32} = f_m h e^{i2\lambda^* ct} \cdot \frac{11}{6\times 42} b^3 F_4(\lambda^*)$; $m_{33} = f_m h e^{i2\lambda^* ct} \cdot \frac{1}{6\times 21} b^4 F_2(\lambda^*)$

$m_{41} = f_m h e^{i2\lambda^* ct} \cdot \frac{13}{112} b^2 F_8(\lambda^*)$; $m_{42} = f_m h e^{i2\lambda^* ct} \cdot \frac{13}{42} b^2 F_{10}(\lambda^*)$

$m_{43} = f_m h e^{i2\lambda^* ct} \cdot \frac{11}{6\times 42} b^3 F_8(\lambda^*)$; $m_{44} = f_m h e^{i2\lambda^* ct} \cdot \frac{13}{42} b^2 F_{12}(\lambda^*)$

$m_{51} = f_m h e^{i2\lambda^* ct} \cdot \frac{13}{42} b^2 F_{14}(\lambda^*)$; $m_{52} = f_m h e^{i2\lambda^* ct} \cdot \frac{13}{42} b^2 F_{16}(\lambda^*)$

$m_{53} = f_m h e^{i2\lambda^* ct} \cdot \frac{11}{6\times 42} b^3 F_{14}(\lambda^*)$; $m_{54} = f_m h e^{i2\lambda^* ct} \cdot \frac{13}{42} b^2 F_{18}(\lambda^*)$

$m_{55} = f_m h e^{i2\lambda^* ct} \cdot \frac{13}{42} b^2 F_{20}(\lambda^*)$; $m_{61} = m_{43}$

$m_{62} = f_m h e^{i2\lambda^* ct} \cdot \frac{11}{6\times 42} b^2 F_{10}(\lambda^*)$; $m_{63} = f_m h e^{i2\lambda^* ct} \cdot \frac{1}{6\times 21} b^4 F_8(\lambda^*)$

$m_{64} = f_m h e^{i2\lambda^* ct} \cdot \frac{11}{6\times 42} b^3 F_{12}(\lambda^*)$; $m_{65} = f_m h e^{i2\lambda^* ct} \cdot \frac{11}{6\times 42} b^3 F_{18}(\lambda^*)$

$m_{66} = f_m h e^{i2\lambda^* ct} \cdot \frac{1}{6\times 21} b^4 F_{12}(\lambda^*)$; $m_{71} = f_m h e^{i2\lambda^* ct} \cdot \frac{9}{6\times 14} b^2 F_2(\lambda^*)$

$m_{72} = f_m h e^{i2\lambda^* ct} \cdot \frac{9}{84} b^2 F_4(\lambda^*)$; $m_{73} = f_m h e^{i2\lambda^* ct} \cdot \frac{13}{6\times 84} b^3 F_2(\lambda^*)$

$m_{74} = f_m h e^{i2\lambda^* ct} \cdot \frac{9}{84} b^2 F_8(\lambda^*)$; $m_{75} = f_m h e^{i2\lambda^* ct} \cdot \frac{9}{84} b^2 F_{14}(\lambda^*)$

$m_{76} = f_m h e^{i2\lambda^* ct} \cdot \frac{13}{6\times 14} b^3 F_8(\lambda^*)$; $m_{77} = m_{11}$

$m_{81} = m_{72}$; $m_{82} = f_{mh} e^{i2\lambda^* ct} \cdot \frac{9}{84} b^2 F_6(\lambda^*)$

$m_{83} = f_{mh} e^{i2\lambda^* ct} \cdot \frac{13}{6\times84} b^3 F_4(\lambda^*)$; $m_{84} = f_{mh} e^{i2\lambda^* ct} \cdot \frac{9}{84} b^2 F_{10}(\lambda^*)$

$m_{85} = f_{mh} e^{i2\lambda^* ct} \cdot \frac{9}{84} b^2 F_{16}(\lambda^*)$; $m_{86} = f_{mh} e^{i2\lambda^* ct} \cdot \frac{13}{6\times84} b^3 F_{10}(\lambda^*)$

$m_{87} = m_{21}$; $m_{88} = m_{22}$; $m_{91} = -m_{73}$; $m_{92} = -m_{83}$

$m_{93} = -f_{mh} e^{i2\lambda^* ct} \cdot \frac{1}{6\times28} b^4 F_2(\lambda^*)$; $m_{94} = -m_{76}$

$m_{95} = -f_{mh} e^{i2\lambda^* ct} \cdot \frac{13}{6\times84} b^3 F_{14}(\lambda^*)$; $m_{96} = -f_{mh} e^{i2\lambda^* ct} \cdot \frac{1}{6\times28} b^4 F_8(\lambda^*)$

$m_{97} = -m_{31}$; $m_{98} = -m_{32}$; $m_{99} = m_{33}$; $m_{10,1} = m_{74}$

$m_{10,2} = m_{84}$; $m_{10,3} = m_{76}$; $m_{10,4} = f_{mh} e^{i2\lambda^* ct} \cdot \frac{9}{84} b^2 F_{12}(\lambda^*)$

$m_{10,5} = f_{mh} e^{i2\lambda^* ct} \cdot \frac{9}{84} b^2 F_{18}(\lambda^*)$; $m_{10,6} = f_{mh} e^{i2\lambda^* ct} \cdot \frac{13}{6\times84} b^3 F_{12}(\lambda^*)$

$m_{10,7} = m_{41}$; $m_{10,8} = m_{42}$; $m_{10,9} = -m_{43}$; $m_{10,10} = m_{44}$

$m_{11,1} = m_{75}$; $m_{11,2} = m_{85}$; $m_{11,3} = f_{mh} e^{i2\lambda^* ct} \cdot \frac{13}{6\times84} b^3 F_{14}(\lambda^*)$

$m_{11,4} = m_{10,5}$; $m_{11,5} = f_{mh} e^{i2\lambda^* ct} \cdot \frac{9}{84} b^2 F_{20}(\lambda^*)$

$m_{11,6} = f_{mh} e^{i2\lambda^* ct} \cdot \frac{13}{6\times84} b^3 F_{18}(\lambda^*)$; $m_{11,7} = m_{51}$; $m_{11,8} = m_{52}$

$m_{11,9} = -m_{53}$; $m_{11,10} = m_{54}$; $m_{11,11} = m_{55}$

$m_{12,1} = m_{94}$; $m_{12,2} = -m_{86}$; $m_{12,3} = m_{96}$; $m_{12,4} = -m_{10,6}$

$m_{12,5} = -m_{11,6}$; $m_{12,6} = -\rho_{mh}\, e^{i2\lambda^* ct} \cdot \frac{1}{6 \times 28}\, b^4 F_{12}(\lambda^*)$;

$F_{12,7} = m_{10,9}$; $m_{12,8} = -m_{62}$; $m_{12,9} = m_{63}$; $m_{12,10} = -m_{64}$

$m_{12,11} = -m_{65}$; $m_{12,12} = m_{66}$

APPENDIX 'B'

TRANSFORMATION MATRICES

$$[a_2]=\begin{bmatrix} O_3 & 1 & & & & & \\ & 01 & & & & & \\ & 001 & & & & & \\ & 0001 & & & & & \\ & 00001 & & & & & \\ & 000001 & & & & & \\ & & O_{18} & 1 & & & \\ & & & 01 & & & \\ & & & 001 & & & \\ & & & 0001 & & & \\ & & & 00001 & & & \\ & & & 000001 & O_{51} & & \end{bmatrix};\quad [a_3]=\begin{bmatrix} O_6 & 1 & & & & & \\ & 01 & & & & & \\ & 001 & & & & & \\ & 0001 & & & & & \\ & 00001 & & & & & \\ & 000001 & & & & & \\ & & O_{21} & 1 & & & \\ & & & 01 & & & \\ & & & 001 & & & \\ & & & 0001 & & & \\ & & & 00001 & & & \\ & & & 000001 & O_{48} & & \end{bmatrix}$$

$$[a_4]=\begin{bmatrix} O_9 & 1 & & & & & \\ & 01 & & & & & \\ & 001 & & & & & \\ & 0001 & & & & & \\ & 00001 & & & & & \\ & 000001 & & & & & \\ & & O_{24} & 1 & & & \\ & & & 01 & & & \\ & & & 001 & & & \\ & & & 0001 & & & \\ & & & 00001 & & & \\ & & & 000001 & O_{45} & & \end{bmatrix};\quad [a_5]=\begin{bmatrix} O_{15} & 1 & & & & & \\ & 01 & & & & & \\ & 001 & & & & & \\ & 0001 & & & & & \\ & 00001 & & & & & \\ & 000001 & & & & & \\ & & O_{30} & 1 & & & \\ & & & 01 & & & \\ & & & 001 & & & \\ & & & 0001 & & & \\ & & & 00001 & & & \\ & & & 000001 & O_{39} & & \end{bmatrix}$$

$$[a_6]=\begin{bmatrix} O_{12} & 1 & & & & & \\ & 01 & & & & & \\ & 001 & & & & & \\ & 0001 & & & & & \\ & 00001 & & & & & \\ & 000001 & & & & & \\ & & O_{33} & 1 & & & \\ & & & 01 & & & \\ & & & 001 & & & \\ & & & 0001 & & & \\ & & & 00001 & & & \\ & & & 000001 & O_{36} & & \end{bmatrix};\quad [a_7]=\begin{bmatrix} O_{21} & 1 & & & & & \\ & 01 & & & & & \\ & 001 & & & & & \\ & 0001 & & & & & \\ & 00001 & & & & & \\ & 000001 & & & & & \\ & & O_{36} & 1 & & & \\ & & & 01 & & & \\ & & & 001 & & & \\ & & & 0001 & & & \\ & & & 00001 & & & \\ & & & 000001 & O_{39} & & \end{bmatrix}$$

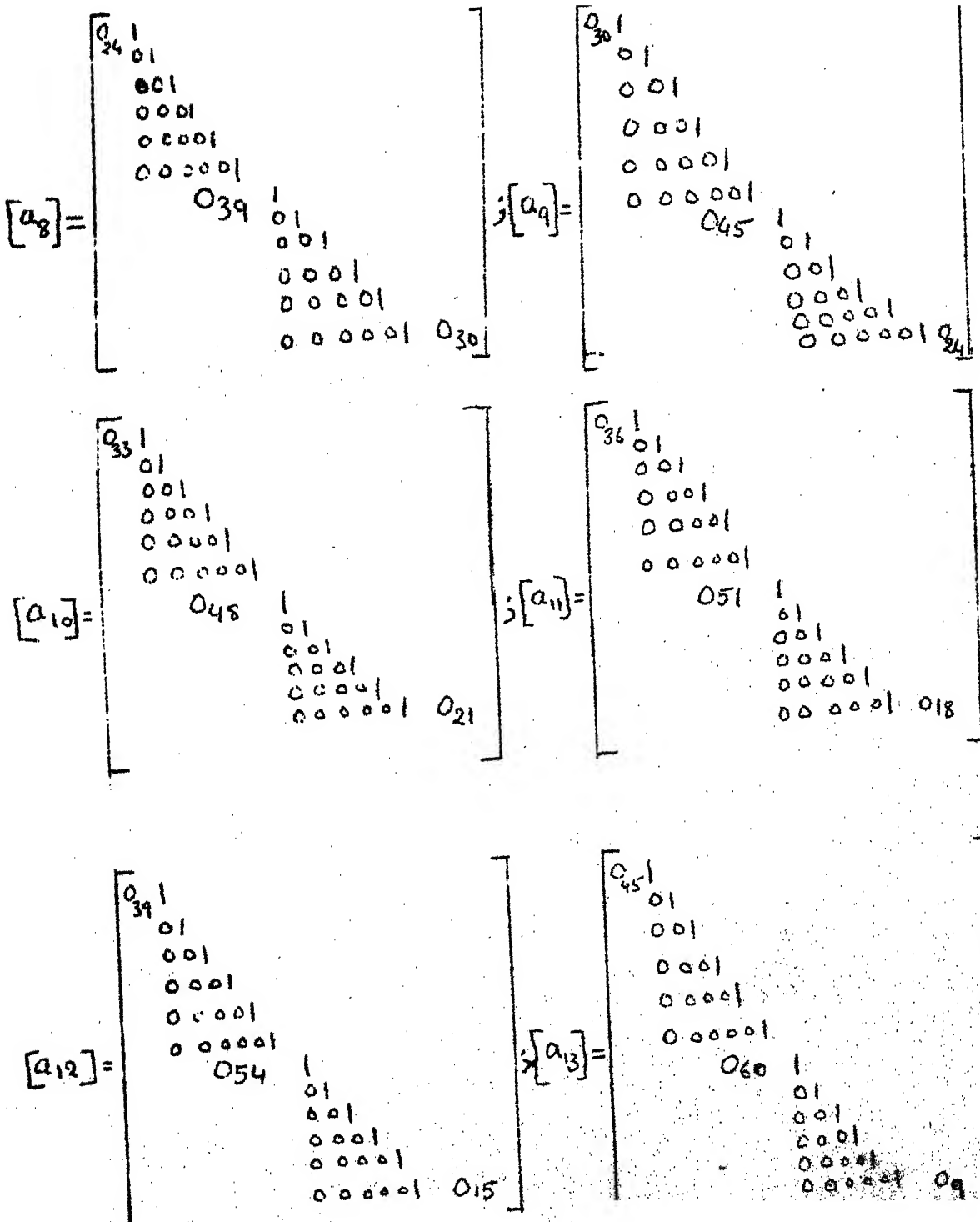

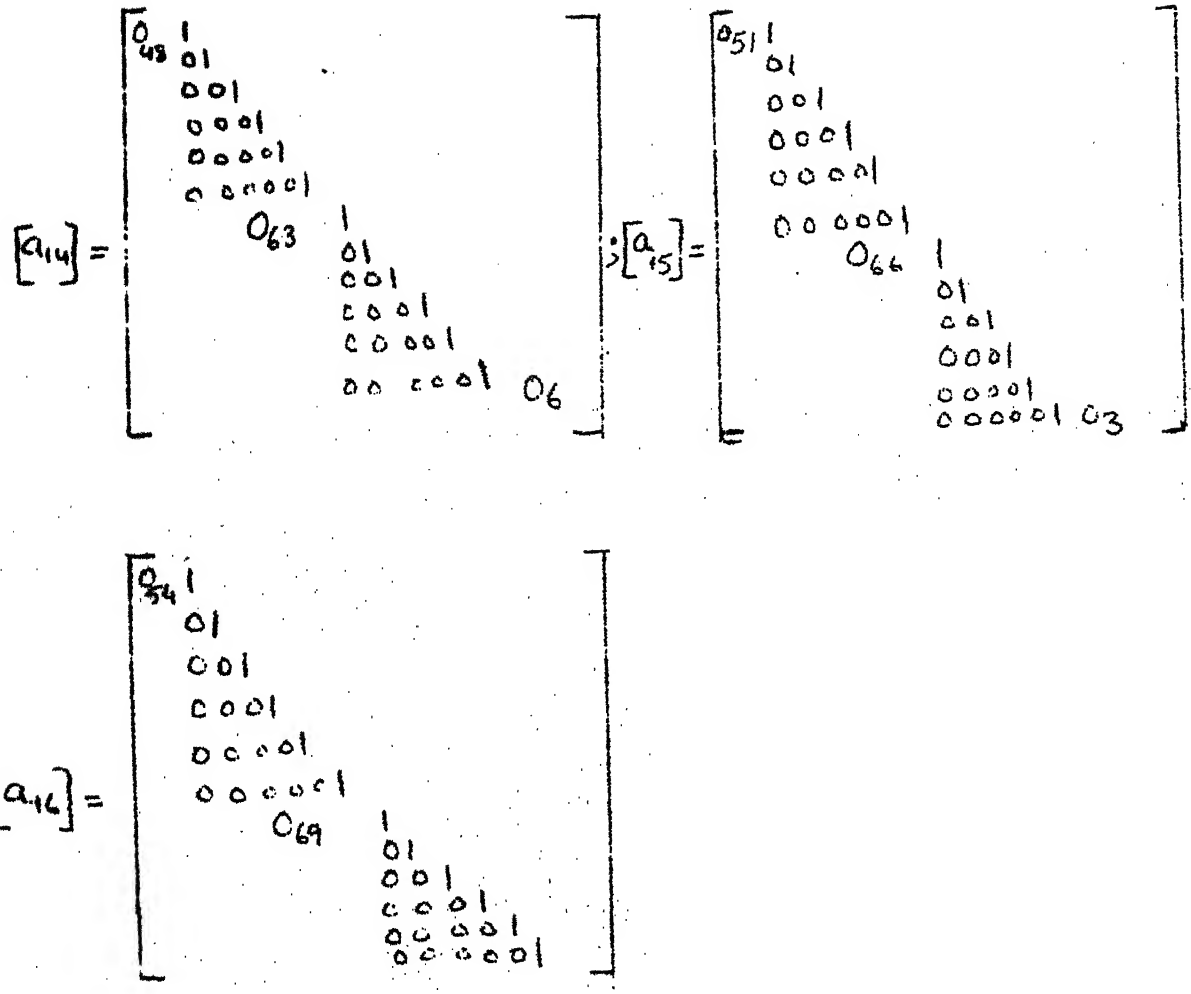

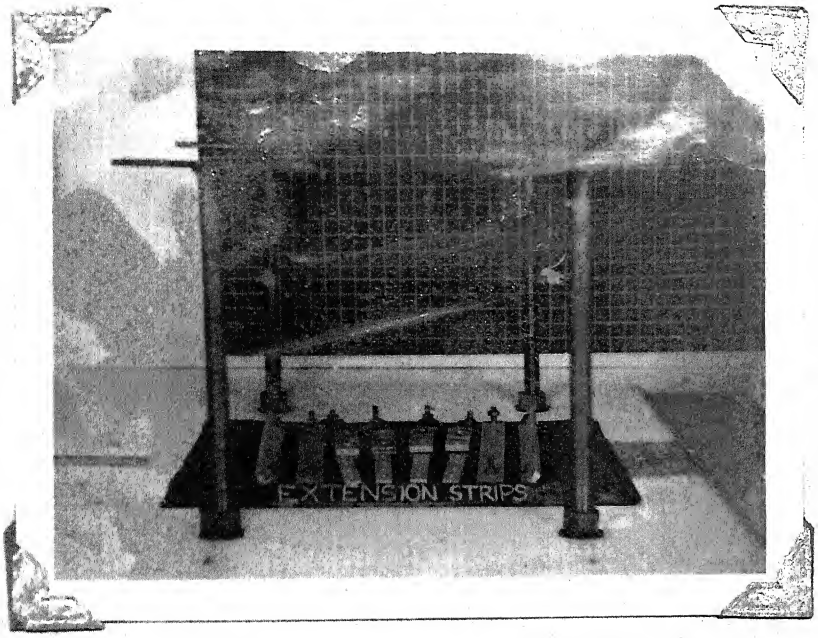

Fig. 2.1 : Membrane Fixture

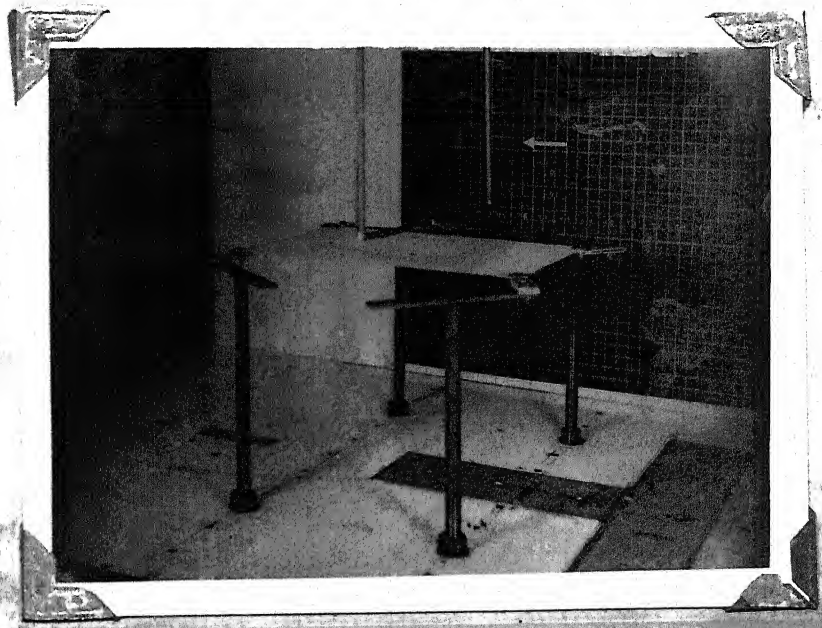

Fig. 2.2 : Pressure Probe on the Membrane

Fig. 2.3:
Pressure Probe Traverse

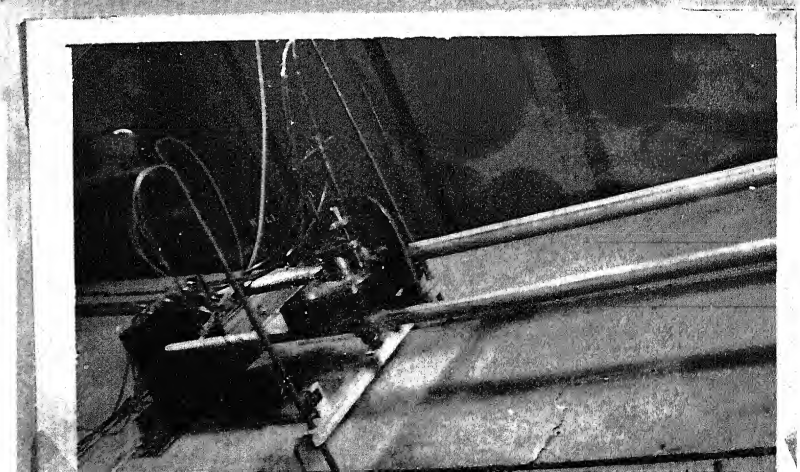

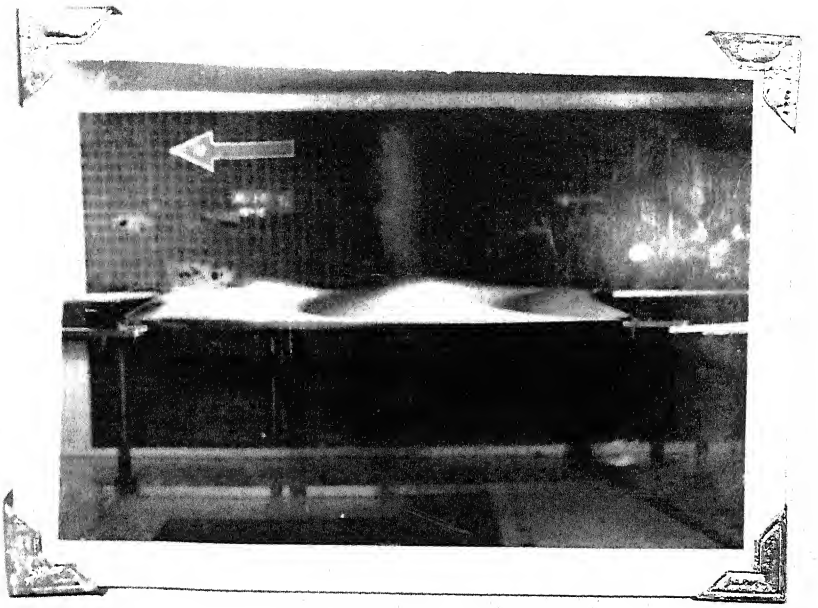

Fig. 2.4 : Large Amplitude Flutter Mode

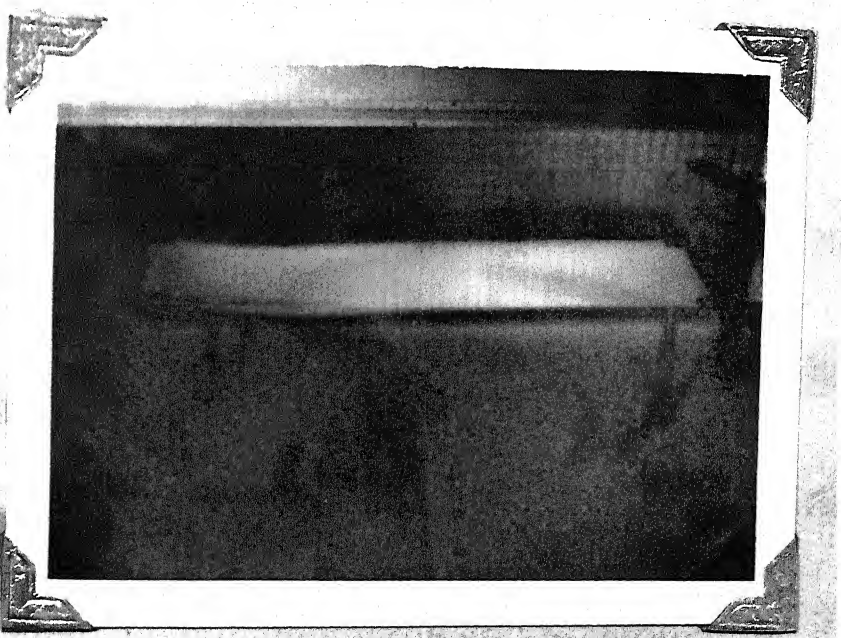

Fig. 2.5 : Low Amplitude Flutter Mode

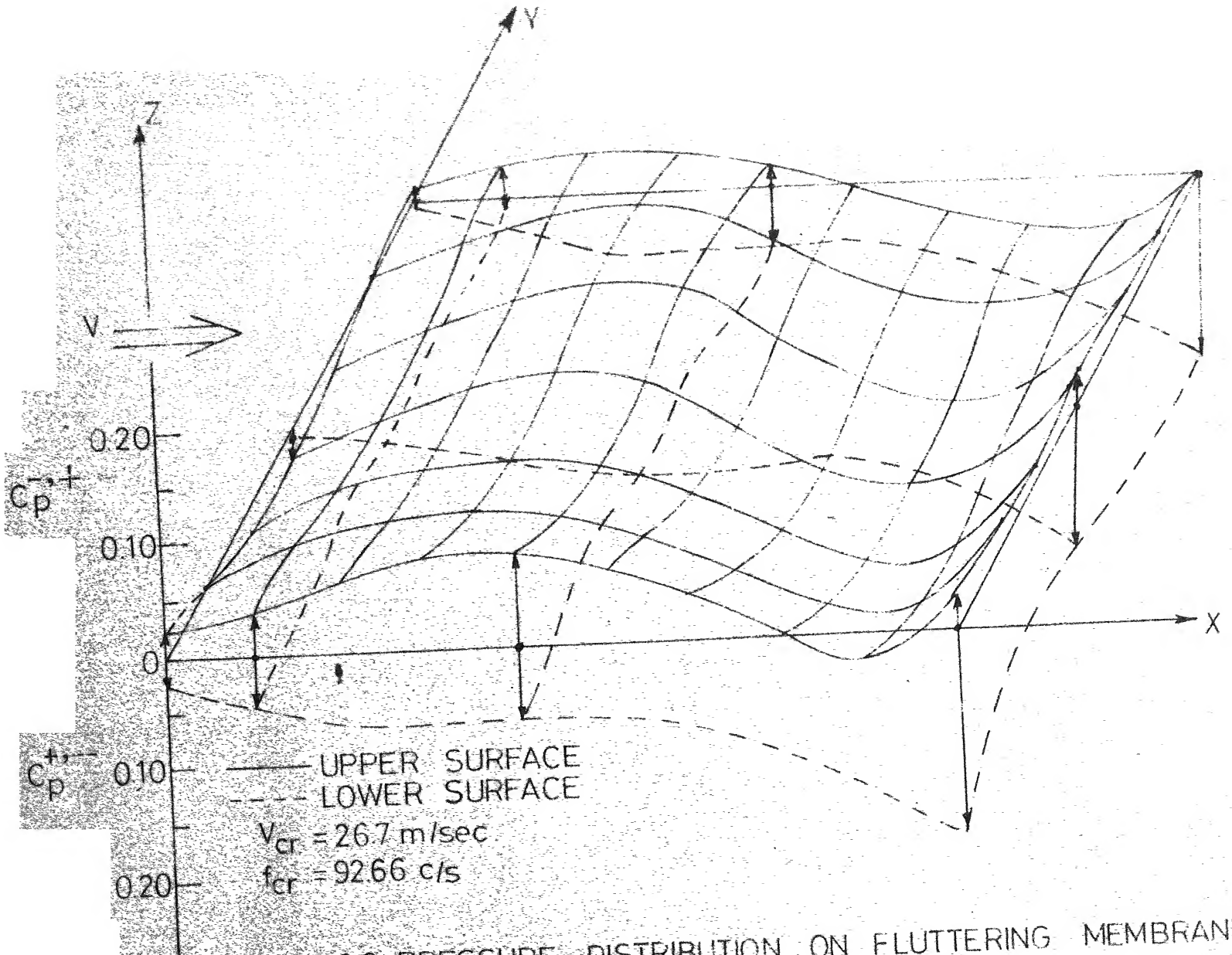

FIG.2.6_PRESSURE DISTRIBUTION ON FLUTTERING MEMBRANE

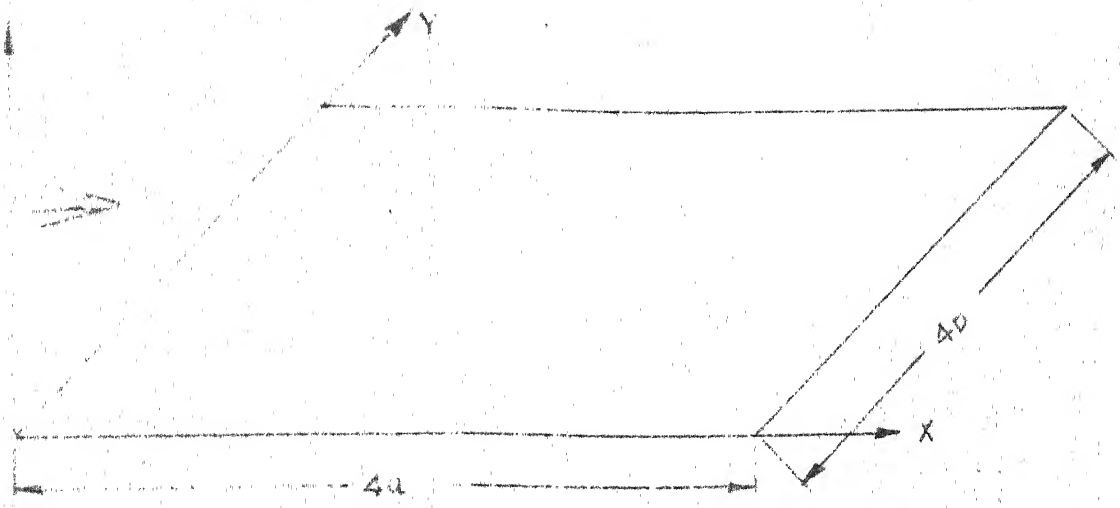

FIG. 3.1 MEMBRANE IN GLOBAL CO-ORDINATE SYSTEM

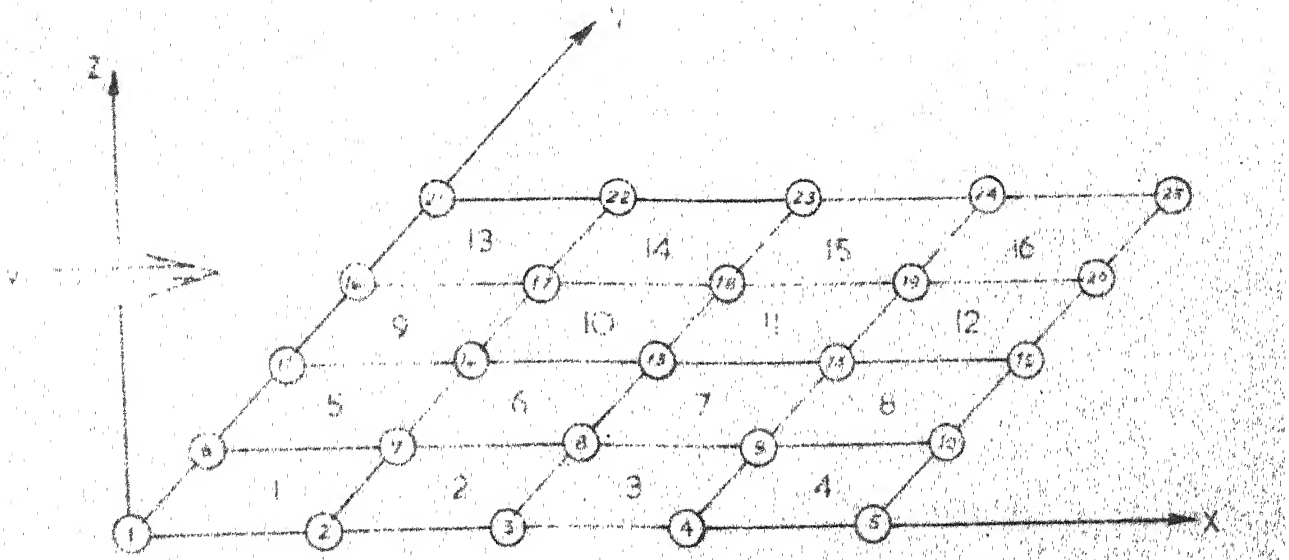

FIG. 3.2 DISCRETIZATION OF MEMBRANE INTO 16-RECTANGULAR ELEMENT

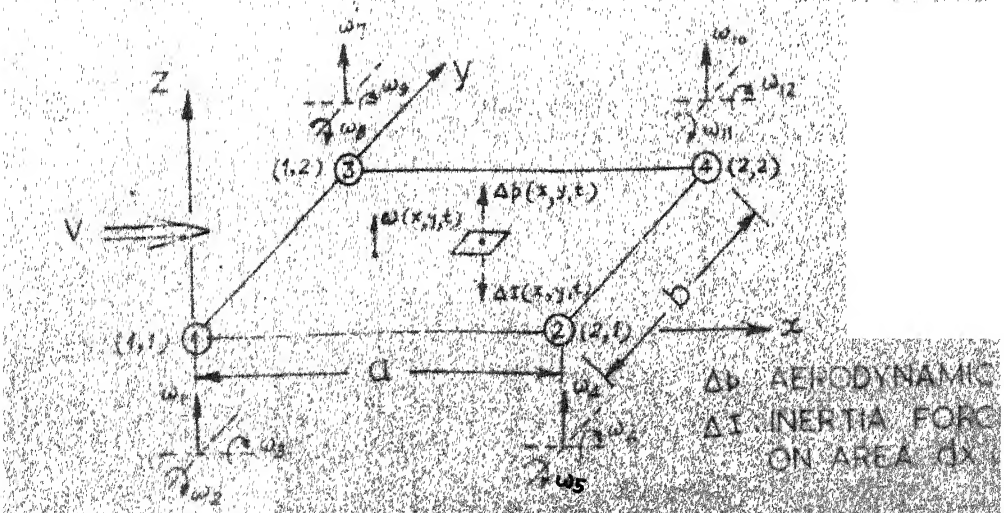

FIG. 3.3 A TYPICAL FINITE ELEMENT IN LOCAL CO-ORDINATE WITH GENERALISED NODAL DISPLACEMENTS

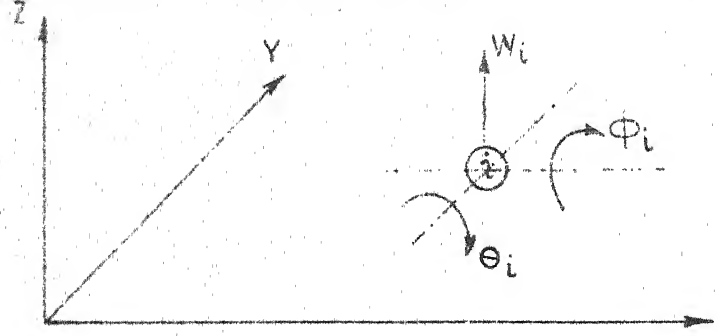

FIG. 5.1_GENERALISED DISPLACEMENTS AT A GLOBAL NODE 'i'

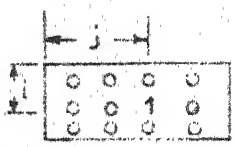

STORING ONLY UNIT ELEMENTS IN 'a_n'

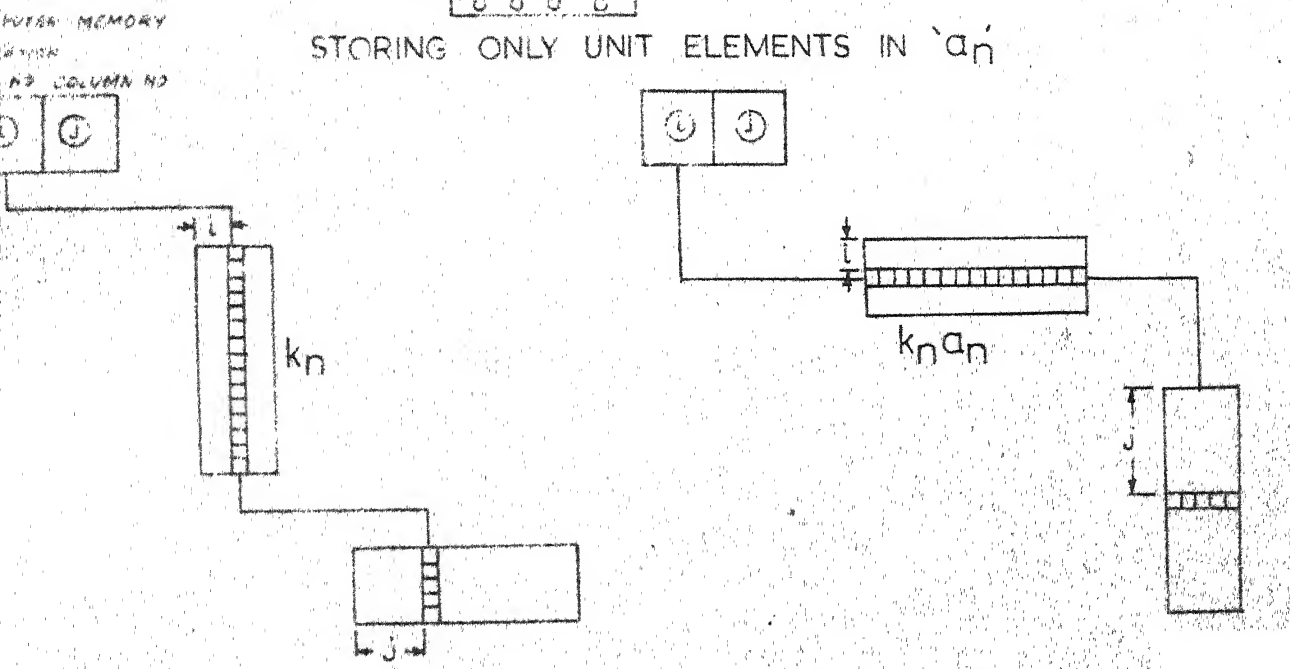

FORMATION OF $k_n a_n$

FORMATION OF K_n

FIG.5.2_FLOW DIAGRAM TO COMPUTE K_n

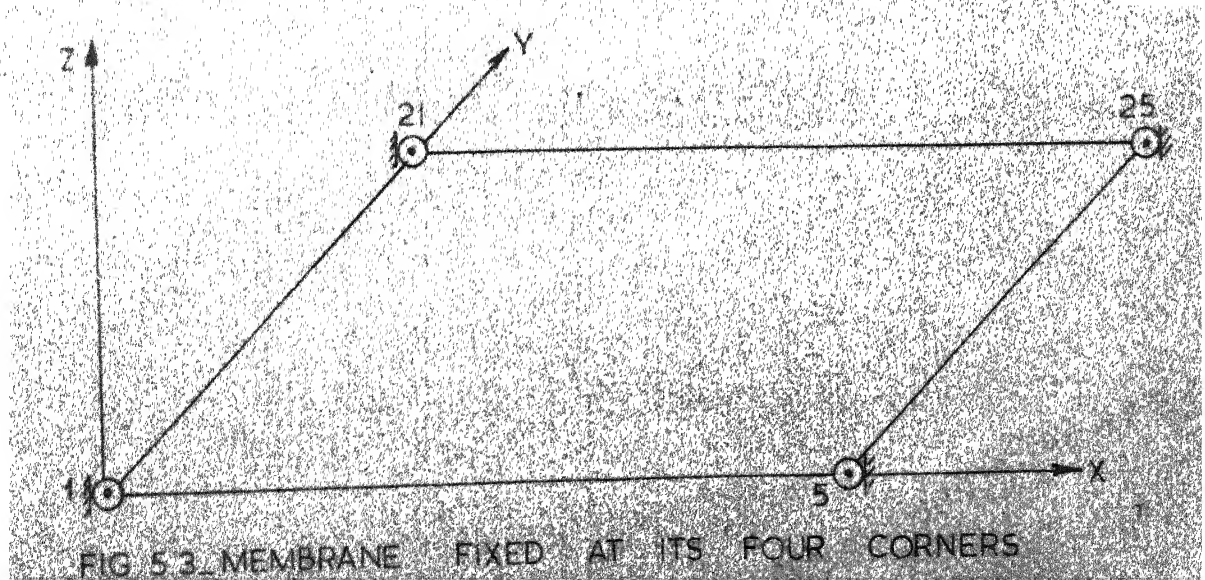

FIG 5.3_MEMBRANE FIXED AT ITS FOUR CORNERS

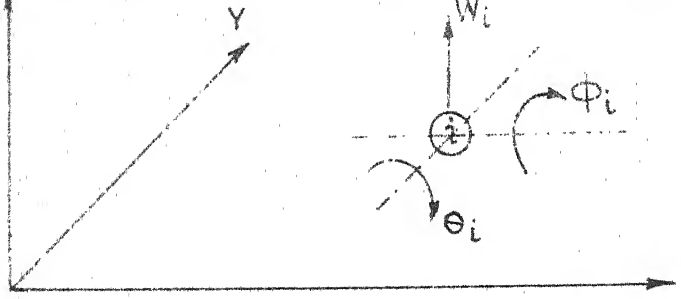

FIG. 5.1_GENERALISED DISPLACEMENTS AT A GLOBAL NODE 'i'

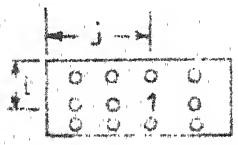

STORING ONLY UNIT ELEMENTS IN 'a_n'

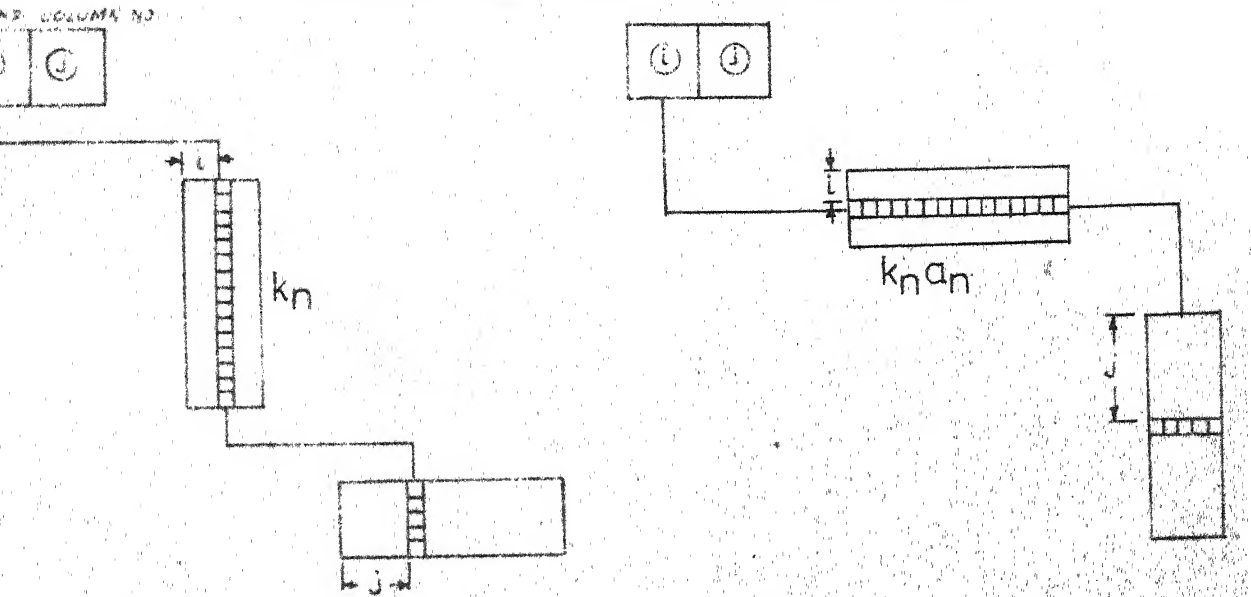

FORMATION OF $k_n a_n$

FORMATION OF k_n

FIG.5.2_FLOW DIAGRAM TO COMPUTE k_n

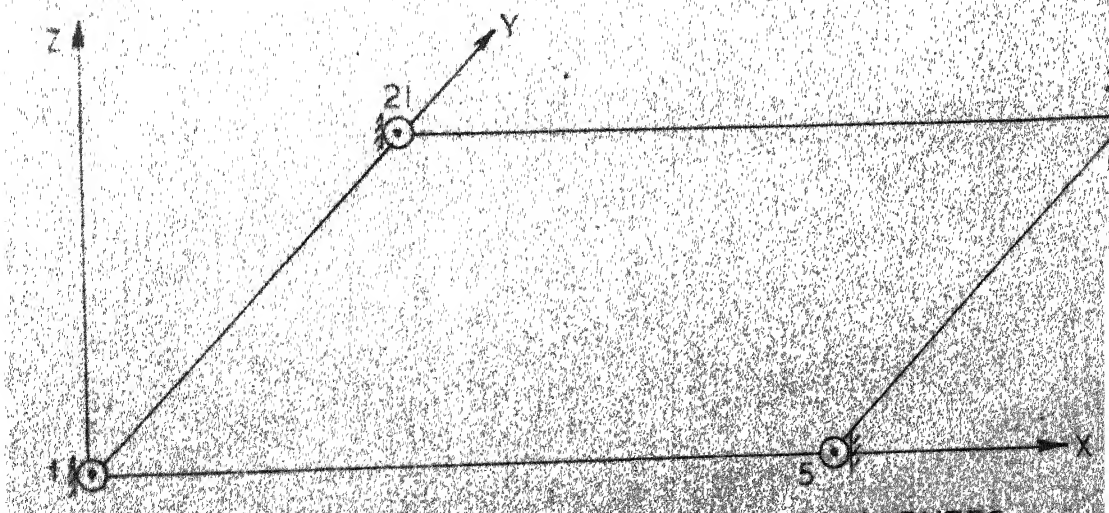

FIG.5.3_MEMBRANE FIXED AT ITS FOUR CORNERS

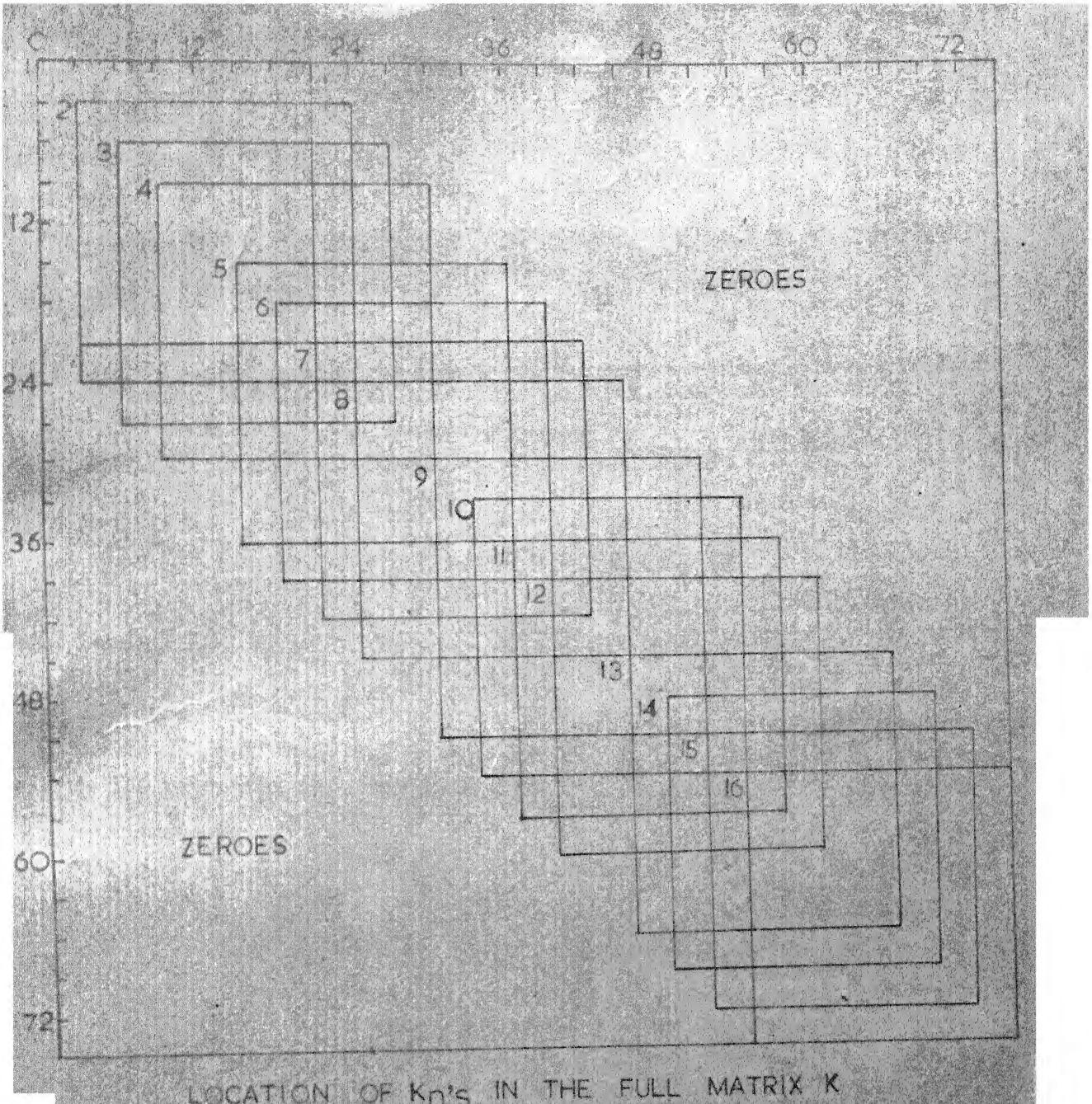

LOCATION OF Kn's IN THE FULL MATRIX K

WHERE n

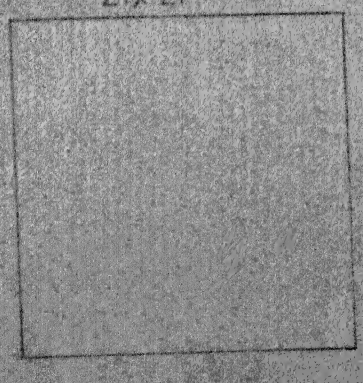

=

n

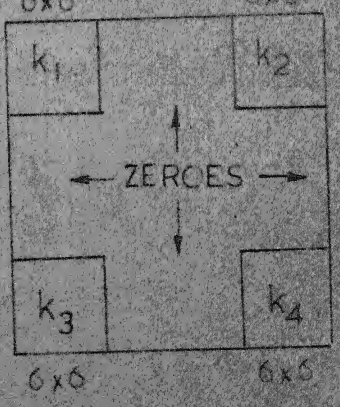

WITH

(k) =

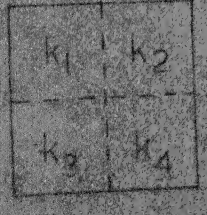

FIG 5.4 ASSEMBLY SCHEME